STUDY OF FISCHER-TROPSCH SYNTHESIS THROUGH THE USE OF SURFACE INTERMEDIATE SCAVENGERS. PROGRESS REPORT, AUGUST 1, 1982-APRIL 1, 1983

TEXAS UNIV. AT AUSTIN

1983

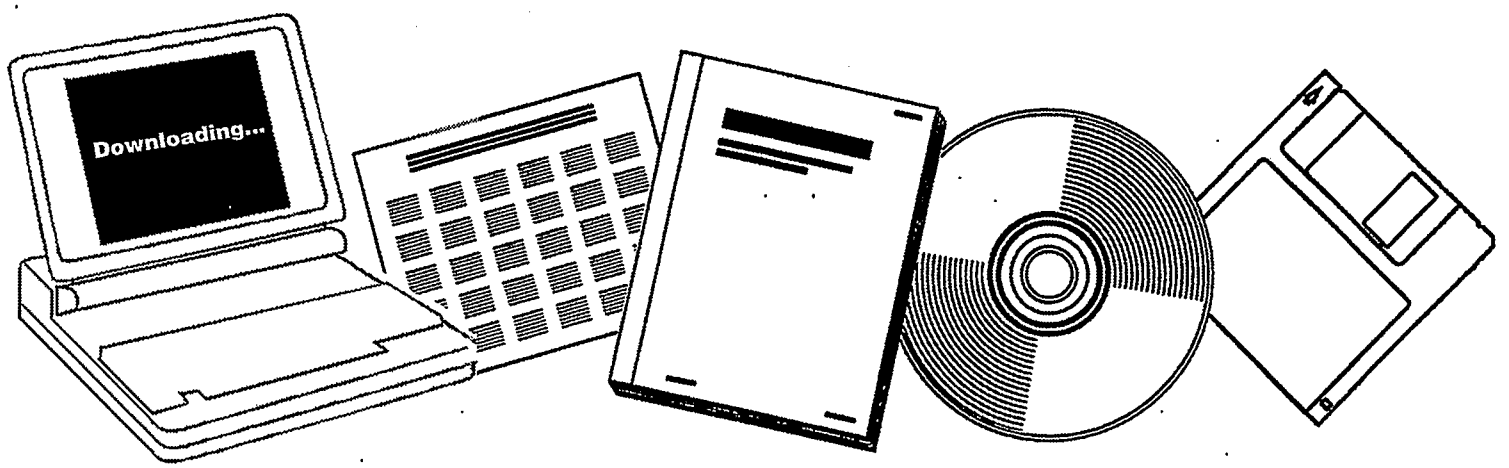

DE83010339

DOE/ER/10720--6

DE83 010339

DOE/ER/10720-6

STUDY OF FISCHER-TROPSCH SYNTHESIS THROUGH THE USE OF SURFACE INTERMEDIATE SCAVENGERS

Progress Report

John G. Ekerdt

The University of Texas

Austin, TX 78712

August 1, 1982 - April 1, 1983

PREPARED FOR THE U.S. DEPARTMENT OF ENERGY

UNDER CONTRACT NO. DE-AS05-80ER10720

ABSTRACT

The primary goal of the research is to identify the reaction pathways by which synthesis gas is converted into hydrocarbons. These mechanisms are needed to understand the fundamental causes for selectivity and to develop more selective catalysts from first principles. The actual effort was directed toward studies of Fischer-Tropsch synthesis over Fe/SiO_2 and isosynthesis catalytic chemistry over ZrO_2.

Fischer-Tropsch synthesis studies concentrated upon the propagation reaction and the role alkyl species have in propagation and termination. Alkyl species concentrations were inferred by scavenging the alkyl species off the surface during Fischer-Tropsch synthesis. Pyridine was used as the scavenger and C_1-C_4-α-Alkylpyridines were formed. The distributions of the alkylpyridines were studied as a function of the synthesis conditions. These studies established that alkyl fragments are the precursor to gas phase products and that alkyl fragments are participating in the propagation reaction. The details of the propagation reaction, methylene versus CO insertion, could not be determined.

Isosynthesis studies concentrated upon the reaction pathway to iso-C_4 products and the initiation of the reaction. Rate measurements at 37 atm suggest that isobutene is formed in a stepwise process between a C_3 carbenium ion and a C_1 oxygenated species. Studies at 1 atm suggest that CO adsorbs and interacts with surface hydroxyl groups to form formates, carbonates and methoxides. The methoxide may be the C_1 species participating in C_4 formation.

INTRODUCTION

The research described herein addresses studies directed toward an understanding of the reaction intermediates and reaction pathways by which synthesis gas is converted into synthetic hydrocarbons. The work was initiated under a grant to investigate the reactive characteristics of alkyl fragments during Fischer-Tropsch synthesis over oxide supported metals. Alkyl fragment distributions were to be determined over a variety of metals by scavenging them from the surface as a means of understanding causes for Fischer-Tropsch selectivity. The experimental scavenging techniques which worked well over Ru (1,2) proved marginal over Fe (3). We sensed that scavenging may not provide the type of information required to discriminate mechanisms and understand causes for reaction selectivity. Scavenging studies continued over Fe and different studies were initiated over ZrO_2 (4,5). Zirconia was investigated because it is inherently selective to C_4 hydrocarbons and understanding the causes for this selectivity might suggest ways to alter the selectivity of other synthesis gas conversion catalysts.

Both research areas rely upon and compliment other research sponsored by DOE's Division of Chemical Sciences into catalytic reaction chemistry and catalytic surface chemistry. A number of projects are investigating the characteristics of transition metal complex ligands which are thought to be intermediates during Fischer-Tropsch synthesis. The initial basis for scavenging was developed from metal complex chemistry (1) and the results, alkyl and alkylidene structures are present on the surface, provide evidence for the existence of these structures as intermediates during Fischer-Tropsch synthesis. More recent work (6) has demonstrated that alkyl fragments are integrally involved in the synthesis reaction.

Studies into the properties of supported metals and reaction kinetics have provided the basis for developing a supported iron catalyst with the extended steady-state activity these studies required and for developing the mechanisms against which to test the alkyl distribution results. Our results are consistent with the mechanisms and suggest the importance of knowing the concentration of reactants responsible for initiation, CO and H, and termination, H. This information will likely come from the spectroscopic and single crystal studies.

Metal oxide catalysis and chemistry of the corresponding organometallic complexes provide the basis for understanding the chemistry of synthesis gas conversion over ZrO_2. These studies indicate how CO is activated and as well as possible surface rearrangements. Zirconia differs from these sytems, however, because it is capable of catalyzing C_2 and higher formation and in a selective manner. Our kinetic and TPD studies demonstrate these differences and future work is expected to suggest causes for the different catalytic properties of ZrO_2 versus ZrO, as an example.

RESEARCH ACCOMPLISHMENTS

Scavenging Studies

The primary objective of the research was to develop a more complete understanding of the reaction intermediates involved in Fischer-Tropsch synthesis by identifying: the reaction intermediates, the means by which they react, and the means by which they are influenced by the synthesis variables. The experimental program included scavenging alkyl species, the postulated intermediates, and rate measurements. In situ infrared work was planned but not carried out because the research focused on Fe which does not adsorb CO in an infrared absorbing state (7,8). The scavenging studies did identify the presence of C_1-C_4 alkyl surface species and measured the influence of the synthesis variables on their distribution. The studies further established that alkyl fragements are intermediates in the Fischer-Tropsch reaction over Fe and participate in chain growth and termination.

The presence of alkyl fragements has been inferred from kinetic studies by postulating mechanisms and showing the correspondence between predicted kinetics and rates, and experimental data. The recent work of Kellner and Bell over Ru is an example of this approach (9). Their study was not based solely on rate measurements; precedence for their mechanism was based on a number of independent studies by other researchers. The presence of alkyl fragments has also been inferred on Ru (1,2) and Fe (3) by reacting a C_xH_y species off the surface and reasoning that the C_xH_y species had to be C_nH_{2n+1}.

Mechanisms have been proposed whereby the alkyl fragments undergo stepwise addition of a C_1 unit. These mechanisms have been described elsewhere (10-12). The two most likely mechanisms are presented in Figure 1. Both involve chain growth steps in which an alkyl fragment undergoes addition.

Methylene Insertion

$$CO_{(g)} \longrightarrow C_{(s)} + CO_{(s)}$$

$$C_{(s)} + H_{(s)} \longrightarrow CH_{(s)} + CH_{2(s)} + CH_{3(s)} + CH_{4(g)}$$

$$CH_{2(s)} + CH_{3(s)} \longrightarrow C_2H_{5(s)}$$

$$CH_{2(s)} + C_2H_{5(s)} \longrightarrow C_nH_{2n+1(s)} \xrightarrow{+CH_{2(s)}}$$

$$C_nH_{2n+1(s)} \xrightarrow{+H_{(s)}} C_nH_{2n+2(g)}$$

$$C_nH_{2n+1(s)} \xrightarrow{-H} C_nH_{2n(g)}$$

CO Insertion

$$CO_{(g)} \longrightarrow C_{(s)} + CO_{(s)}$$

$$C_{(s)} + H_{(s)} \longrightarrow CH_{3(s)} + CH_{4(g)}$$

$$CH_{3(s)} + CO_{(s)} \longrightarrow COCH_{3(s)} \xrightarrow{H_{(s)}} C_2H_{5(s)} + H_2O$$

$$C_2H_{5(s)} + CO_{(s)} \longrightarrow COC_2H_{5(s)} \xrightarrow{H_{(s)}} C_nH_{2n+1} \xrightarrow{+CO_{(s)}}$$

$$C_nH_{2n+1} \xrightarrow{+H_{(s)}} C_nH_{2n+2(g)}$$

$$C_nH_{2n+1} \xrightarrow{-H} C_nH_{2n(g)}$$

FIGURE 1

Variations of each mechanism have been published, the basic features are that during methylene insertion alkyl fragments form directly with each propagation step (9). The CO insertion reaction proceeds from an alkyl to an acyl, which upon hydrogenation and dehydration produces an alkyl fragment (12). Both mechanisms share common termination steps in which an alkyl fragment undergoes hydride elimination to an olefin or hydrogenation to an alkane (9).

The research was based on the assumptions that alkyl fragments are involved in the propagation reaction and that the dependence of the alkyl fragment distributions on the partial pressure of reactants, H_2 and CO, should be different for either mechanism. Experiments were performed to scavenge alkyl fragments, to establish that alkyl fragments are precursors to stable gas phase products, and to determine the effect of synthesis conditions on alkyl surface distributions. This was accomplished by continuously adding a low concentration of pyridine to the reactant feed gas and collecting the reactor effluent for later analysis. Pyridine reacted with alkyl fragments on the iron surface. The catalyst used throughout the studies was 20.4 wt% Fe_2O_3/SiO_2 which converted into Fe_3O_4, Fe and carbides under synthesis conditions (3).

The analytical problems for this research were formidable. Pyridine was used as a scavenger because it contains a heteroatom which can not be formed from CO and H_2. Attempts with cyclic hydrocarbons produced inconclusive results because iron catalyzed the formation of the cyclic hydrocarbons which were anticipated upon scavenging alkyl fragments with cyclohexene or benzene. α-Alkyl-substitutedpyridines, C_1-C_4-pyridines, were formed at very low concentrations which have retention times in capillary columns close to Fischer-Tropsch products. A Nitrogen-Phosphorus Detector (NPD) was used

because it is insensitive to the Fischer-Tropsch hydrocarbon products. Finally, the capillary column used, carbowax on amine deactivated fused silica, was extremely unstable and sensitive to deactivation by oxygen or H_2O, a Fischer-Tropsch product.

Figures 2-7 are representative of the data collected at 230°C (6). Figures 2 and 3 present methane rate data prior to and during scavenging as well as the concentration of methylpyridine. These figures demonstrate that pyridine suppresses the rate but does not alter the surface reactions because the dotted lines are parallel to the dashed lines. The reactant partial pressure dependences for methylpyridine are similar for CO, negative, and less positive for H_2. Similar plots are presented elsewhere for ethyl- and propylpyridine (6). Figures 4 to 7 present the pressure dependences of the ratio of C_{n+1}-pyridine/C_n-pyridine and the rates of formation of Fischer-Tropsch products n+1/n. These figures demonstrate that alkyl fragments are integrally involved in the formation of Fischer-Tropsch products. The ratio of $\frac{C_{n+1}\text{-pyridine}}{C_n\text{-pyridine}}$ should be proportional to the ratio of alkyl fragments on the catalyst surface during Fischer-Tropsch synthesis.

The central question is whether the partial pressure dependences of the alkylpyridines enable one to establish the mechanism, methylene insertion versus CO insertion. Langmuir-Hinshelwood rate expressions were constructed for both mechanisms. These were used to predict the concentration of alkyl fragments. Predicted alkyl distributions were compared against experimental aklylpyridine distributions. The details and arguments are lengthy and will not be presented here, merely the results.

The Langmuir-Hinshelwood expressions for each mechanism generate chain growth parameters, α, which are given by

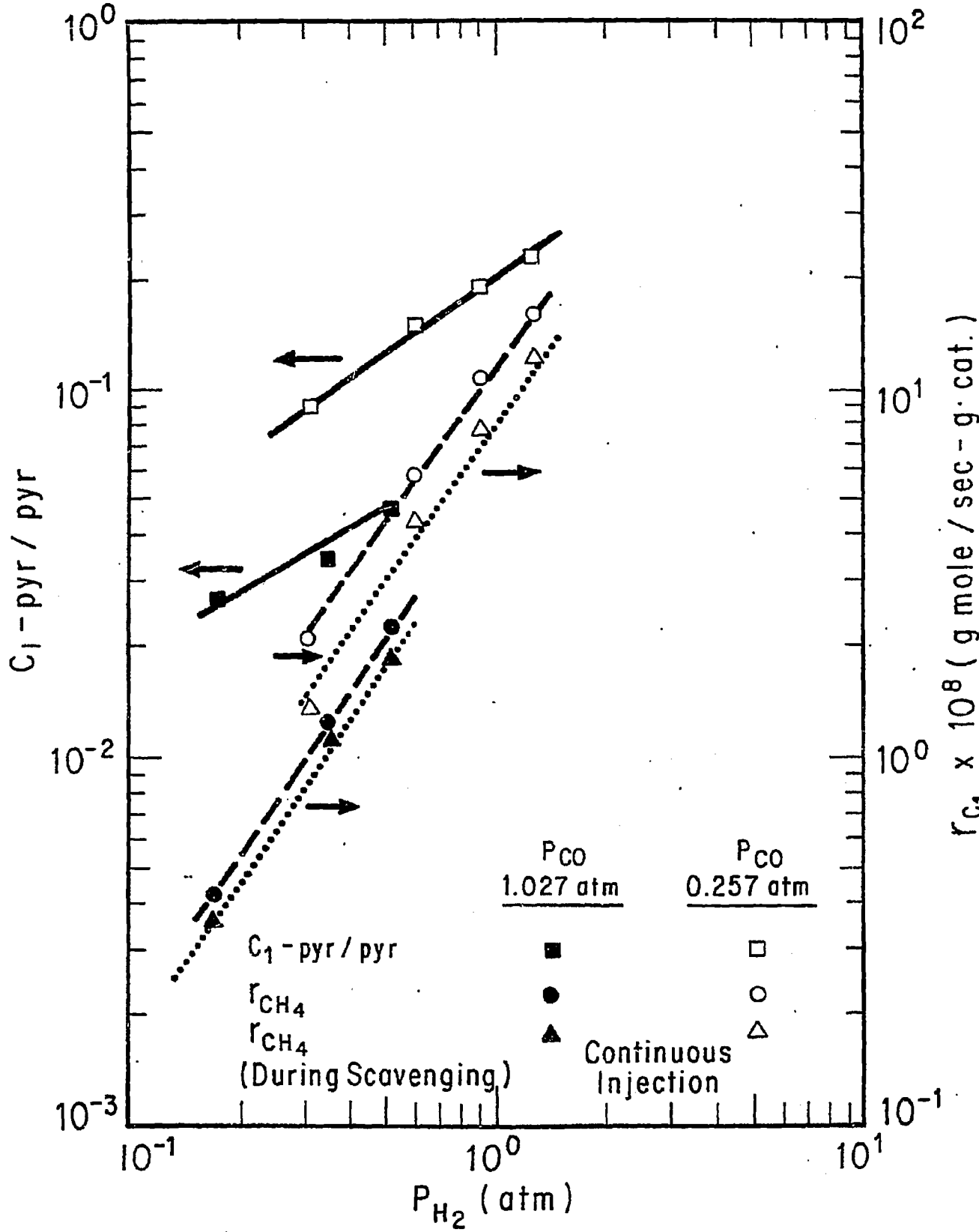
10^0
10^{-1}
10^{-2}
10^{-3}
10^2
10^1
10^0
10^{-1}
C_1 - pyr / pyr
r_{C_1} x 10^8 (g mole / sec - g · cat.)
10^{-1}
10^0
10^1
P_{H_2} (atm)
P_{CO} 1.027 atm
P_{CO} 0.257 atm
C_1 - pyr / pyr
r_{CH_4}
r_{CH_4} (During Scavenging)
Continuous Injection

FIGURE 2

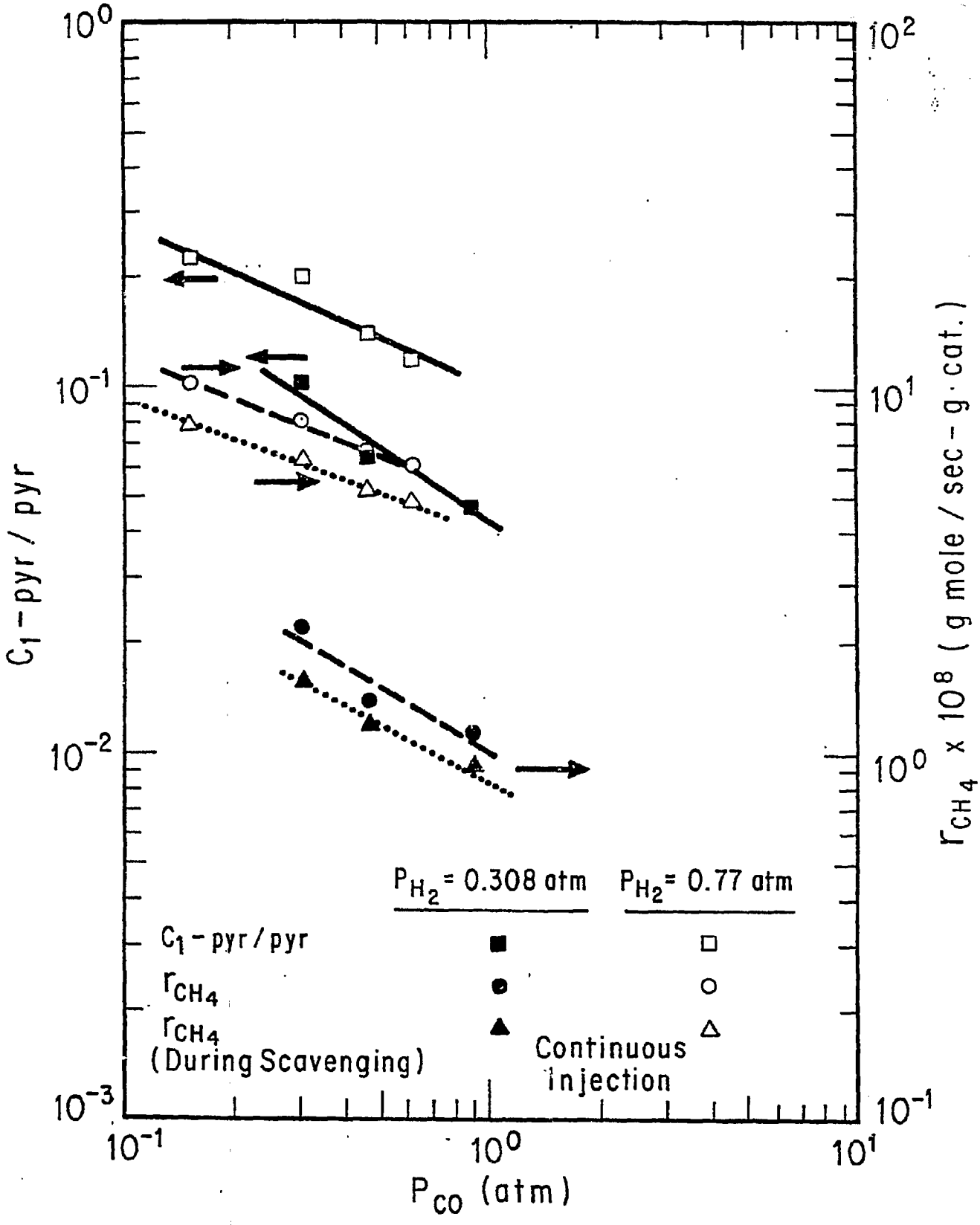
10^0
10^{-1}
10^{-2}
10^{-3}
10^2
10^1
10^0
10^{-1}
10^{-1}
10^0
10^1
C_1 - pyr / pyr
r_{CH_4} x 10^8 (g mole / sec - g · cat.)
P_{CO} (atm)
P_{H_2} = 0.308 atm
P_{H_2} = 0.77 atm
C_1 - pyr / pyr
r_{CH_4}
r_{CH_4} (During Scavenging)
Continuous injection

FIGURE 3

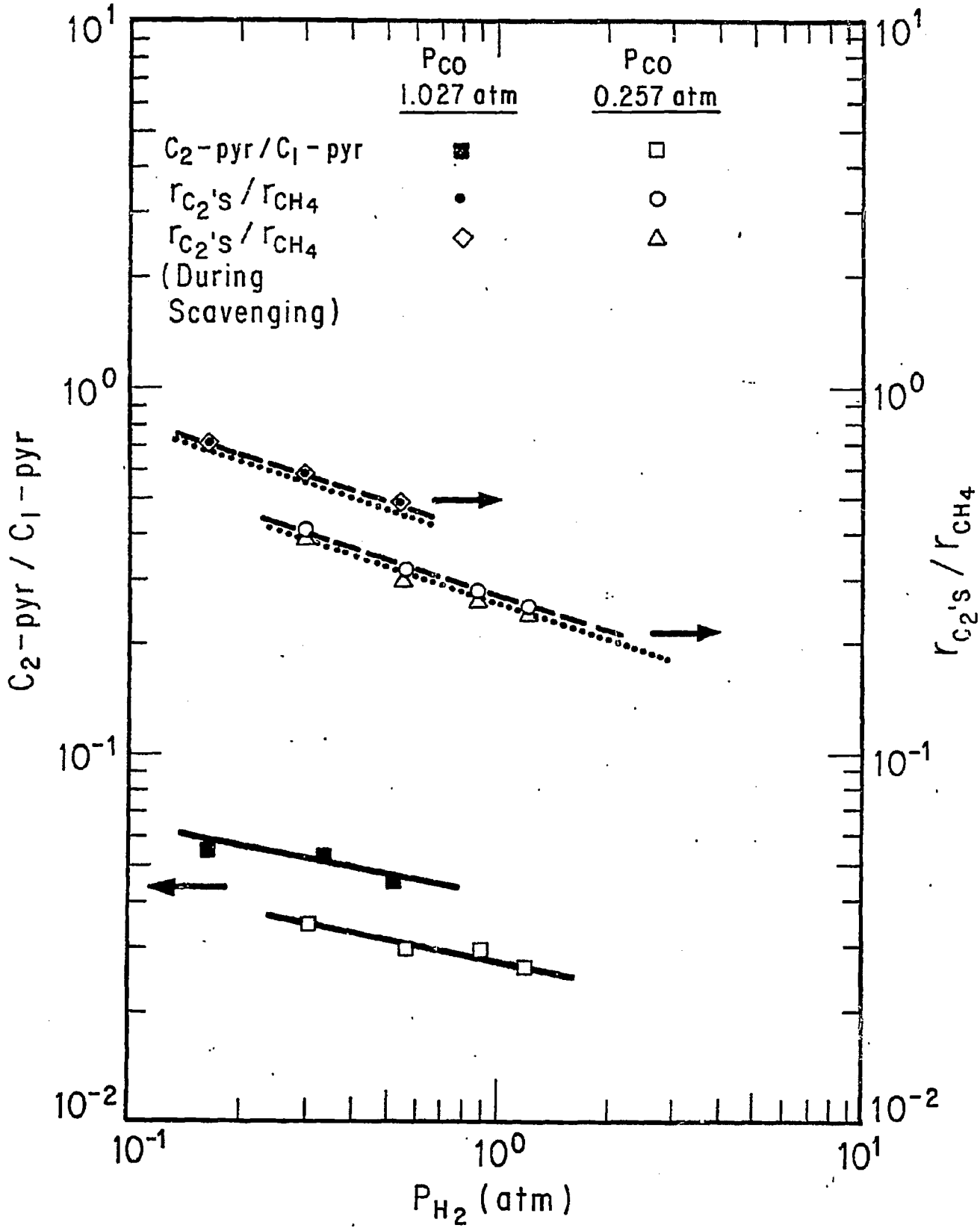
P_{CO} 1.027 atm
P_{CO} 0.257 atm
C_2-pyr / C_1-pyr
$r_{C_2's} / r_{CH_4}$
$r_{C_2's} / r_{CH_4}$ (During Scavenging)
C_2-pyr / C_1-pyr
$r_{C_2's} / r_{CH_4}$
P_{H_2} (atm)
10^1
10^0
10^{-1}
10^{-2}

FIGURE 4

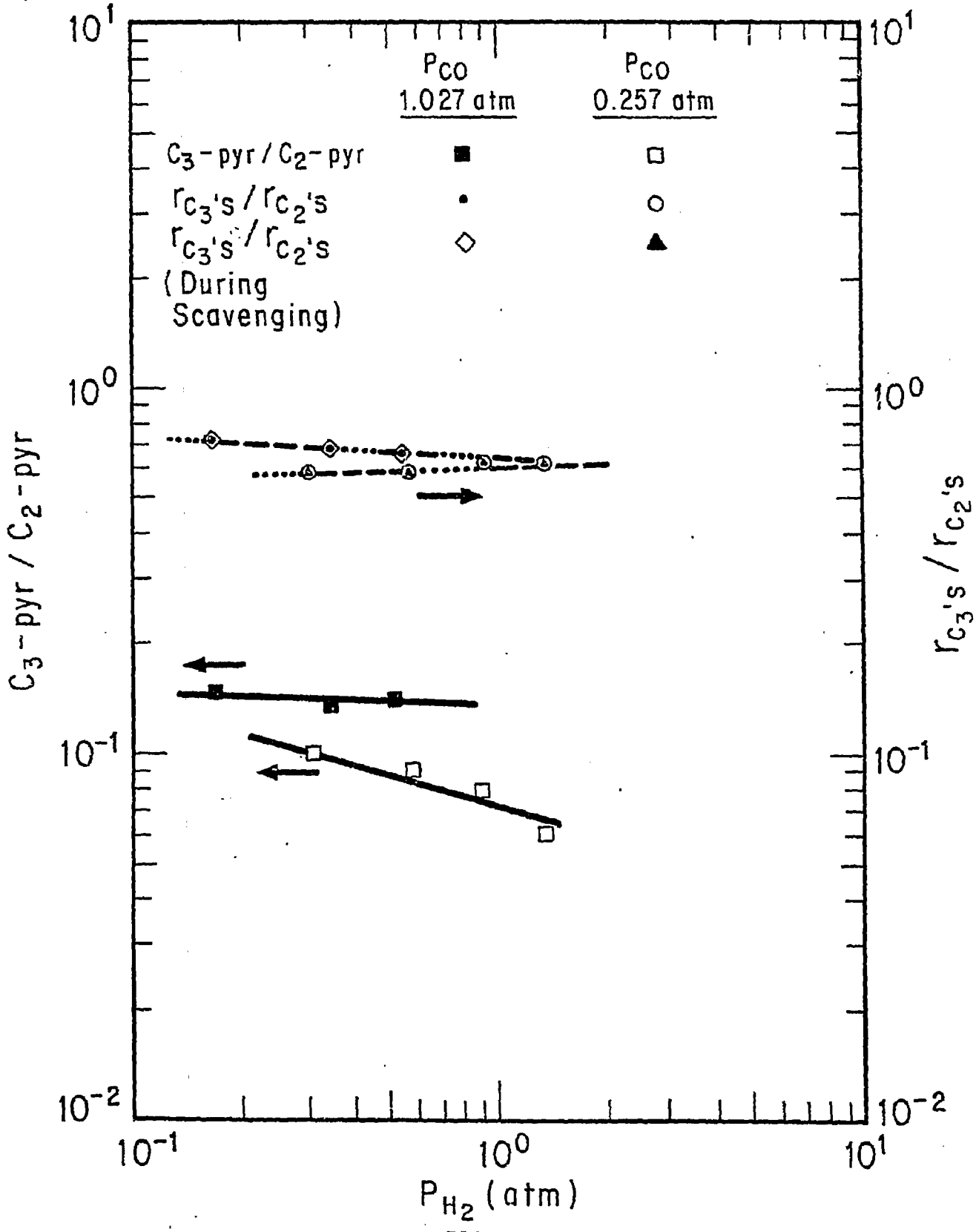
P_{CO} 1.027 atm
P_{CO} 0.257 atm
C_3 - pyr / C_2 - pyr
$r_{C_3's} / r_{C_2's}$
$r_{C_3's} / r_{C_2's}$ (During Scavenging)
C_3 - pyr / C_2 - pyr
$r_{C_3's} / r_{C_2's}$
P_{H_2} (atm)
10^1
10^0
10^{-1}
10^{-2}

FIGURE 5

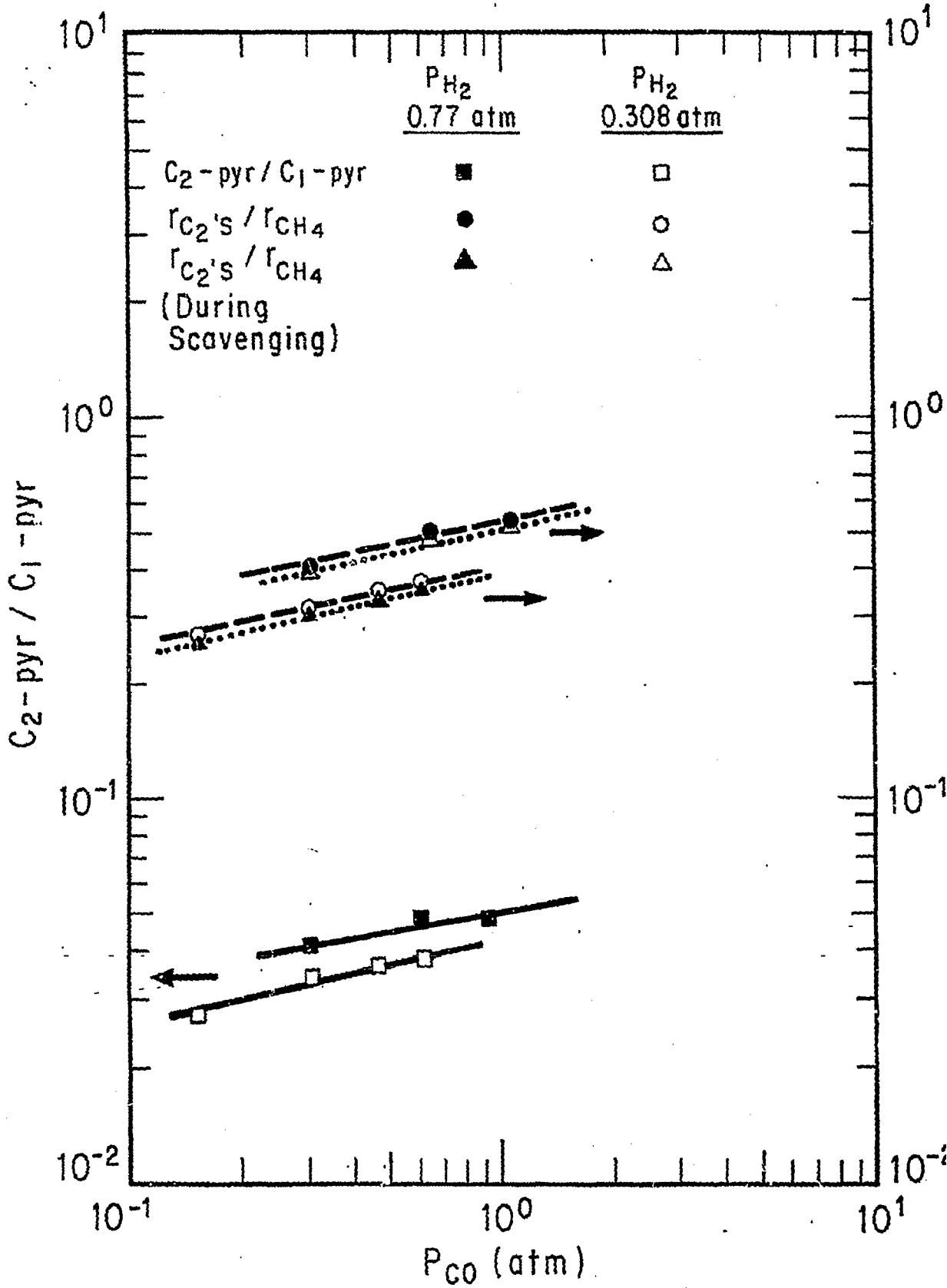
P_{H_2} 0.77 atm
P_{H_2} 0.308 atm
C_2 - pyr / C_1 - pyr
$r_{C_2's} / r_{CH_4}$
$r_{C_2's} / r_{CH_4}$ (During Scavenging)
C_2 - pyr / C_1 - pyr
P_{CO} (atm)
10^1
10^0
10^{-1}
10^{-2}

FIGURE 6

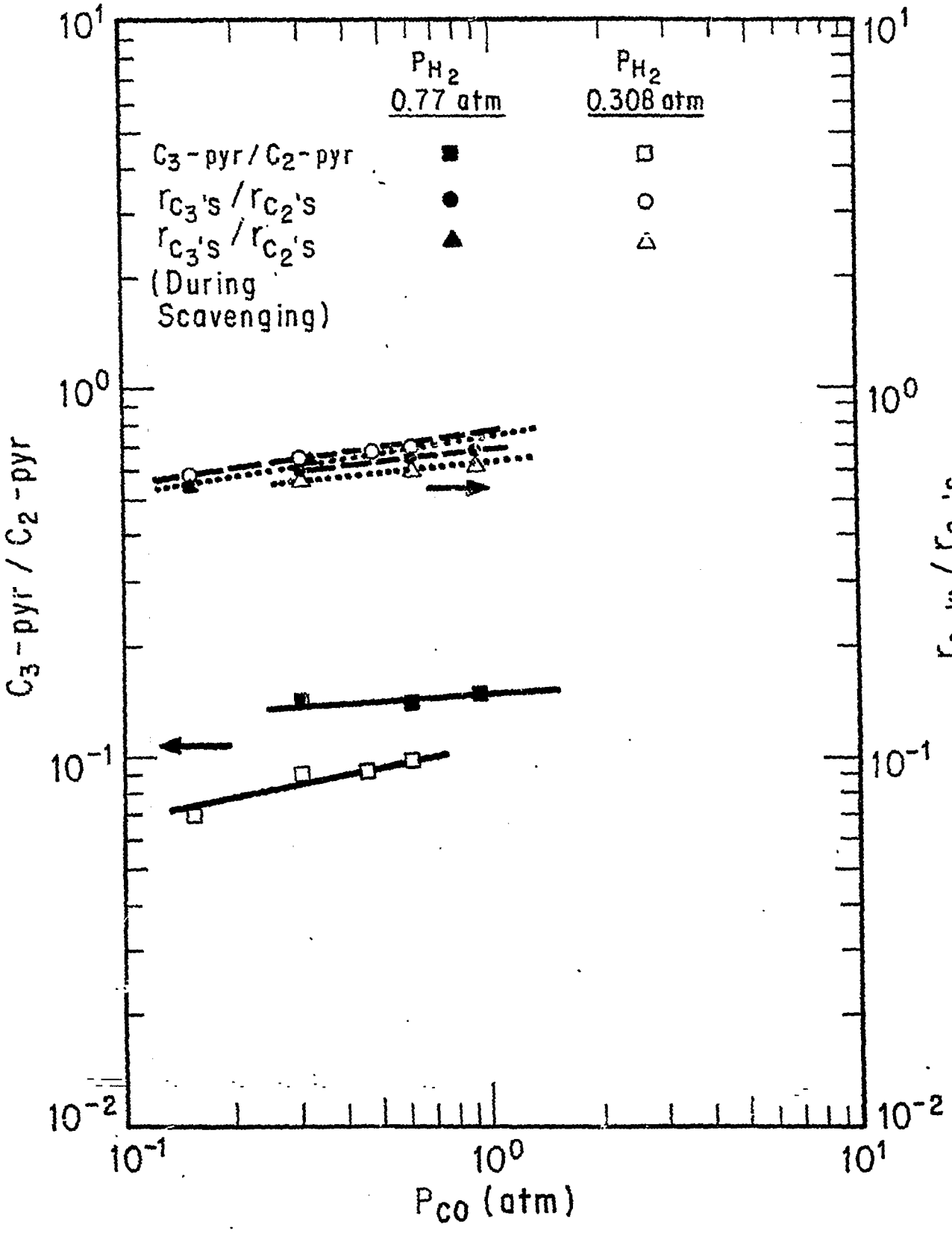
P_{H_2} 0.77 atm
P_{H_2} 0.308 atm
C_3 - pyr / C_2 - pyr
$r_{C_3's} / r_{C_2's}$
$r_{C_3's} / r_{C_2's}$ (During Scavenging)
C_3 - pyr / C_2 - pyr
$r_{C_3's} / r_{C_2's}$
P_{CO} (atm)
10^1
10^0
10^{-1}
10^{-2}

FIGURE 7

$$\alpha = \frac{\theta_{n+1}}{\theta_n} = \frac{\text{rate of propagation}}{\text{rate of propagation + rates of termination}} , \qquad (1)$$

where θ_n is the fraction of surface sites covered by the alkyl fragment C_nH_{2n+1}. The expressions were sorted for the coverage of θ_n, θ_H, θ_{CO}, and θ_{vacant}. The P_{CO} dependence was unknown. It was not possible to assume CO saturated the surface (8) as it does over Ru (9). A negative P_{CO} dependence of unknown magnitude was assumed for θ_{vacant}. This was assigned the value of β. The results of this analysis are presented in Table 1.

The ratios of θ_{n+1}/θ_n are given by α. The ratios C_2-pyridine/C_1-pyridine and C_3-pyridine/C_2-pyridine are expected to be proportional to the concentrations of θ_1 to θ_3. Therefore, the ratios of alkylpyridine signals shown in Figures 4-7 should have the same partial pressure dependences as does α. The results are summarized in Table 2, where a negative hydrogen and positive carbon monoxide dependence are observed.

The expressions in Table 1 were examined in the limits where propagation was much greater than termination ($\alpha = 1$) and where termination dominated ($\alpha = 0$). These results are given in Table 3. The actual value for α could not be determined for our experiments; however, a value between 0.4 and 0.7 is expected (13,14). This implies that the actual partial pressure dependences will be intermediate between those shown in Table 3.

The results in Table 2 demonstrate that the hydrogen dependence was negative and of order 0.2. Both mechanisms predict a negative P_{H_2} dependence reasonably close to this value. The experimental partial pressure ratio for P_{CO} was of positive order 0.2. Both mechanisms predict a value which is positive. The unknown θ_V dependence, β, is bounded by one and zero. For

Table 1. Partial Pressure Dependences for the Chain Growth Parameter

Methylene Insertion:

$$\alpha \propto \frac{k_p \dfrac{P_{H_2}^{0.4}}{P_{CO}^{0.5-\beta(a)}}}{k_p \dfrac{P_{H_2}^{0.4}}{P_{CO}^{0.5-\beta}} + k_o \dfrac{1}{P_{CO}^{\beta}} + k_A \dfrac{P_{H_2}^{0.5}}{P_{CO}^{\beta}}}$$

CO Insertion

$$\alpha \propto \frac{k_I P_{CO}^{1}}{k_I P_{CO}^{1} + k_o + k_A P_{H_2}^{0.5}}$$

(a) $0 < \beta < 1$

Table 2. Partial Pressure Dependence for Alkylpyridine Ratios

Ratio $\frac{C_{n+1}\text{-pyr}}{C_n\text{-pyr}}$	P_{CO} (atm)	P_H (atm)	Nominal H_2/CO range	x(a)	y(a)
2/1	1.027		0.2-0.5		-0.19
2/1	0.257		0.7-5		-0.20
2/1		0.770	1 - 5	0.17	
2/1		0.308	0.2-1	0.22	
3/2	1.027		0.2-0.5		-0.03
3/2	0.257		0.7-5		-0.27
3/2		0.770	1 - 5	0.07	
3/2		0.308	0.2-1	0.17	

(a) x and y are defined as $C_{n+1}\text{-pyr}/C_n\text{-pyr} = gP_{CO}^{x}P_{H_2}^{y}$

Table 3 Predicted Partial Pressure Dependences for α at the Extremes

	Mechanism	P_{CO}	P_{H_2}
$\lim\alpha \to 1$	Methlene Insertion	0	0
$\lim\alpha \to 1$	CO Insertion	0	0
$\lim\alpha \to 0$	Methylene Insertion	$2\beta - 0.5$	-0.1
$\lim\alpha \to 0$	CO Insertion	1	-0.5

values of β greater than 0.25 the methylene insertion mechanism predicts smaller values for the P_{CO} dependence.

More information is required about CO adsorption and coverage at reaction conditions over iron catalysts before a value of β can be determined. Without this value it is not possible to discriminate between the mechanisms by measuring the partial pressure dependences of the reaction intermediates. This probably results from the fact that both mechanisms share common intermediates and common termination steps.

The scavenging technique did work. Alkyl fragment distributions were observed and were found to depend upon synthesis conditions. These dependences were not unique enough to enable mechanism discrimination over Fe.

Scavenging studies are in progress over Ru wich pyridine. Ruthenium has a higher probability for chain growth than does iron. In addition, the CO coverage dependence is well documented. We are interested in scavenging C_5 and higher fragments and in determining if chain length affects the rates of propagation. These studies will be completed by the end of the contract period.

Isosynthesis Studies

The primary objectives of the isosynthesis studies were to identify the reaction pathways to branched hydrocarbons and to understand the causes for the selective conversion over ZrO_2. Because very little information is reported for isosynthesis (15-18) and most of this refers to ThO_2 (15-17), rate studies were conducted to investigate the effects of synthesis conditions on the C_4 isomers. A differential fixed-bed reactor, operated at 37 atm, was used. The objective was to collect steady-state rate data which could be used as the basis for proposing surface reactions. The details of

this effort are described in Appendix I (4). Studies at 1 atm were directed toward understanding how CO and H_2 interact over ZrO_2 and characterizing the types of resulting intermediates.

The rate studies can be summarized as follows. Isobutene was the major product. The distribution of branched/normal C_4's remained constant with residence time and temperature suggesting skeletal rearrangement of the products was not occurring. Increasing the residence time or temperature increased the alkane/olefin distribution and the degree of isomerization of 1-butene into the internal olefins. These results strongly suggest that iso- and 1-butene are the primary C_4 products and that they are formed from a common intermediate by stepwise addition of a C_1 species to a C_3 species.

The reaction mechanism was not revealed by the rate studies. Arguments were presented (4) for a possible mechanism which are based upon mechanisms postulated for the methanol conversion over the acid centers of ZSM-5 (19-24). The most probable seems to be $X\text{-}OCH_3$, X = H, CH_3 or Zr, adds to a C_3 carbenium ion. The secondary carbenium ion would be more stable and would lead to the preferred product isobutene. If OCH_3 is added O would be removed by dehydration which is probably catalyzed by the basic sites of ZrO_2.

These studies are continuing in a different differential reactor. A new reactor has been fabricated with a copper liner to suppress the blank activity of the stainless tube surface. This will enable us to examine the C_1 to C_3 products in more detail and determine if isosynthesis occurs between gas/phase and surface species in Eley-Rideal type fashion or if C_2 and higher species are formed and remain on the surface until they terminate as a stable product. The details of this work are discussed in the renewal proposal.

The studies at 1 atm were directed toward understanding how CO and H_2 interact over ZrO_2. Temperature programmed techniques were used to investigate the adsorption/desorption and decomposition of CO, H_2, methanol, D_2O and formic acid. The experiments were performed in the apparatus shown in Figure 8. Two grams of ZrO_2 (Alfa 98.9% 1-3 μ spheres with a BET area of 5.8 m^2/g) was placed in a quartz reactor tube. The tube was continually flushed with an inert or reactive gas. The reactor effluent was sampled continuously with a UTI 100 C mass spectrometer.

A typical experiment involved heating ZrO_2 to 620°C in flowing O_2 and maintaining it at 620°C for 0.5 hr (O_2, 620°, 0.5) followed by a helium flush for 0.25 min (He, 620°, 0.25) and a hydrogen flush for 0.25 min (H_2, 620°, 0.25). The reactor was purged of H_2 and the adsorbing gas was passed over the catalyst as the catalyst was cooled to 25°C. This was done to give ample opportunity for the different structures, which may only form at high temperature, to form. The carrier gas, referred to as flushing gas, was changed to the desired mixture and the catalyst was heated at a linear rate of 1°C/sec.

Signals were measured for nine masses. The instrument was calibrated according to the procedure of Ko et al. (25). Pulses of known amounts of CO were directed to the mass spectrometer and the corresponding signal was assigned to a number of molecules. All other species were related to this intensity (25). The molecules detected were divided by the BET surface area present in the reactor. Data will be presented which show molecules/nm^2. These should not be interpreted as absolute, rather as representative of the relative amounts of each species. They are more meaningful than, strong, very strong, weak, etc.

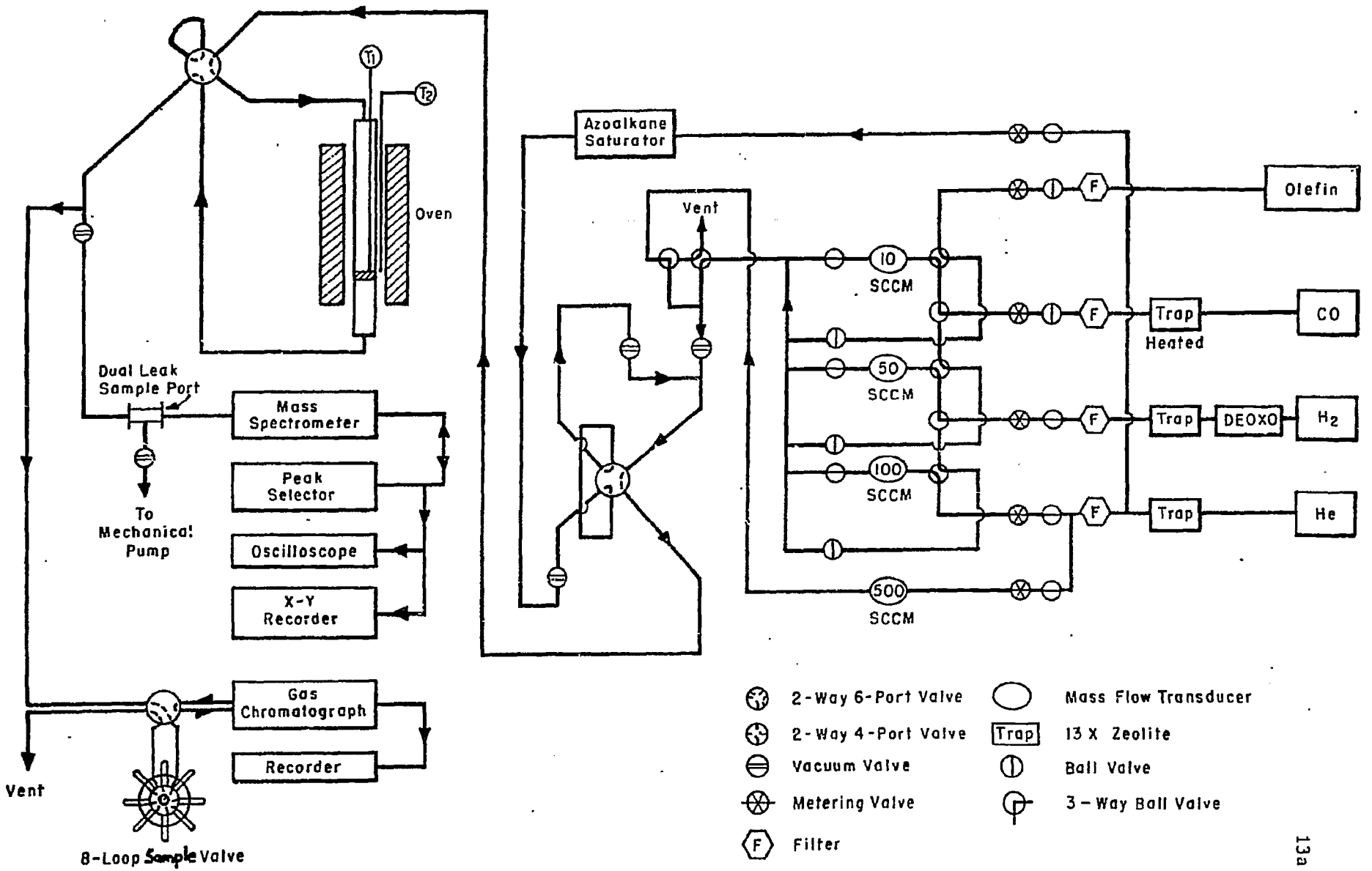
T1
T2
Oven
Dual Leak
Sample Port
Mass
Spectrometer
Peak
Selector
Oscilloscope
X-Y
Recorder
To
Mechanical
Pump
Gas
Chromatograph
Recorder
Vent
8-Loop Sample Valve
Azoalkane
Saturator
Vent
10
SCCM
50
SCCM
100
SCCM
500
SCCM
F
Olefin
Trap
Heated
CO
Trap
DEOXO
H2
Trap
He
2-Way 6-Port Valve
2-Way 4-Port Valve
Vacuum Valve
Metering Valve
Filter
Mass Flow Transducer
Trap
13 X Zeolite
Ball Valve
3-Way Ball Valve

FIGURE 8

Selected results from Temperature Programmed Desorption (TPD) and Temperature Programmed DEcomposition (TPDE) of adsorbed species are presented in Tables 4-6. The species were detected in five distinct temperature ranges:

α - 40-60°C ;

β - 120-180°C ;

γ - 380-420°C ;

δ - 460-510°C ;

ε - 580-620°C .

These results can be used to answer or suggest answers to the following questions: 1) what surface intermediates form upon adsorption of synthesis gas; 2) how are these intermediates formed; and, 3) what is the interaction between CO, H_2 and the intermediates on the surface? The manuscript for a paper which discusses this work is in preparation (5); detailed arguments for our interpretation are still being formulated. These interpretations will be substantiated with FT-IR studies which will be initiated under the current contract and are proposed for the renewal proposal.

Only CO is observed at the α temperature. We interpret this to be weakly adsorbed molecular CO.

Both CO and CO_2 are observed at the β temperature, with CO_2 as the predominant species. Adsorbed or gas phase CO was converted into CO_2, and adsorbed CO_2 did generate a small amount of CO. This suggests that CO and CO_2 are formed via the same intermediate. For CO to CO_2 this also suggests that surface oxygen atoms or ions of ZrO_2 are involved in the formation of the intermediate. The likely structure is a bidentate carbonate.

The surface intermediate which decomposed at the γ temperature produced mainly CO. We suspect it may be a different bidentate carbonate from that

Table 4. TPD and TPDE of CO, H_2, and CO/H_2 on ZrO_2

No	ZrO_2 Treatment	Preadsorbate 620-25°C	Flushing Gas	Product	Molecules/nm^2				
					α	β	γ	δ	ε
I	O_2,620°	CO	He	CO	0.31		0.04		
	H_2,620°			CO_2		1.56			
II	O_2,620°	CO	H_2	CO	0.15		0.17	0.08	
	H_2,620°			CO_2		0.99			
				CH_4				0.21	
III	O_2,620°	H_2	He	H_2					0.26
	H_2,620°								
IV	O_2,620°	H_2	CO	CO_2		0.47			0.45
	H_2,620°			H_2					0.41
V	O_2,620°	CO/H_2	He	CO	0.07	0.01	0.51	0.20	
	H_2,620°			CO_2		0.82			
				CH_4				0.10	
				H_2				0.26	0.20
VI	O_2,620°	CO/H_2	CO/H_2	CO_2		0.53			3.13
	H_2,620°			CH_4				0.27	
VII	O_2,620°	none	CO/H_2	CO_2		0.39			0.82
	H_2,620°			CH_4					0.05

Table 5. TPD and TPDE of CO_2, HCOOH, and CH_3OH

No	ZrO_2 Treatment	Preadsorbate (temperature)	Flushing Gas	Product	Molecules/nm^2				
					α	β	γ	δ	ε
I	O_2,620°	CO_2	He	CO		0.10	0.12		
	H_2,620°	(620-25°)		CO_2		0.57			
II	O_2,620°	none	CO_2/H_2	CO					2.56
	H_2,620°			CH_4					0.06
III	O_2,620°	CO_2/H_2	H_2	CO		0.06	0.06		
	H_2,620°	(620-25°)		CO_2		0.30			
				CH_4				0.05	
IV	O_2,620°	HCOOH	He	CO			6.54		0.26
		(25°)		CO_2			1.35		0.32
				CH_4			0.02		0.15
				H_2			0.17		0.07
				H_2O			3.17		
				H_2CO			0.03		
V	O_2,620°	CH_3OH	He	CO		0.46		2.23	
		(25°)		CO_2				0.05	
				CH_4		1.68		2.01	
				H_2				3.25	
				H_2O				0.48[a]	

(a) Broad peak which covered the range ε and δ

Table 6. TPD and TPDE of CO and CO/H_2 on ZrO_2 by Pulse Preadsorption

No	ZrO_2 Treatment	Preadsorbate (temperature)	Flushing Gas	Product	Molecules/nm^2				
					α	β	γ	δ	ε
I	O_2,620°	CO	He	CO			0.03		
	H_2,620°	(320°)		CO_2			0.05		
II	O_2,620°	CO/H_2	He	CO				0.41	0.14
	H_2,620°	(320°)		CO_2				0.07	0.20
				CH_4				0.17	0.22
III	O_2,620°	CO/H_2	He	CO				0.26	0.22
	H_2,620°	(520°)		CO_2					0.26
				CH_4				0.10	0.23
				H_2				0.37	0.74

which decomposed at the β temperature. Two kinds of bidentate carbonate have been reported on ZrO_2 following CO_2 adsorption (26). The structures are shown below

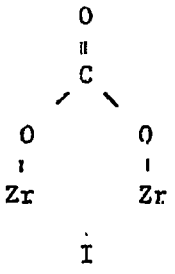

I

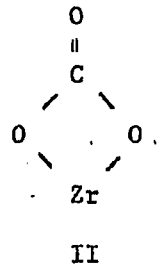

II

Structure II was more stable than I and decomposed at higher temperatures (26). Carbonates also formed on ThO_2 when CO was adsorbed (27,28). It seems reasonable to suggest that if structures I and II are present, structure I decomposed at the β temperature and structure II at the γ temperature.

Bidentate carbonates have been observed over TiO_2 upon adsorption of CO_2 or CO (29,30). The bidentate carbonate was argued to form via a bicarbonate. The TPDE of a bicarbonate should give rise to CO_2 and/or CO and H_2O, which was never observed at the β or γ temperatures. This may suggest that carbonates form via a different route over ZrO_2.

The TPDE of methanol produced CO, CO_2, CH_4, H_2, and H_2O at the δ temperature. Methane is also observed at this temperature when both CO and H_2 are present. Comparison of Table 4-V and 5-V reveals that the products are ranked $H_2 > CO > CH_4$. This combined with other experimental data suggests that a methoxide (methoxy) species decomposed at the δ temperature.

Formic acid decomposed at two temperatures, γ and ε. The predominance of CO and H_2O at the γ temperature suggests that formic acid underwent dehydration at the γ temperature. Carbon dioxide was the major component at the ε temperature sugesting that a different species was decomposing at this temperature. Methane is also observed at the ε temperature. Formate or

formate ion are thought to be the species giving rise to products at the ε temperature.

Adsorption of CO/H_2 at 320°C and 520°C revealed that methane was generated at the δ and ε temperatures upon subsequent TPD/TPDE. This implies that 320°C is sufficient to form the methoxide and formate. Adsorption at 520°C was followed by flushing with He and cooling to 25° under He. Again methane was formed at the δ and ε temperatures. This suggests that the ε structure, formate, can be converted into the δ structure, methoxide.

Additional experiments were performed over a surface which was partially covered with OD species. Carbon monoxide was adsorbed and subjected to TPD/TPDE under flowing CO. Some CD_4 and CHD_3 were observed. Sequential experiments were performed with the same catalyst without reconditioning with O_2 and H_2. Upon successive TPD/TPDE cycles less CO_2 and CH_4 were observed at the ε temperature. Addition of D_2O at 320°C restored the activity to that seen in the first TPD/TPDE. These results suggest that OH or OD groups are responsible for formate and methoxide formation.

The mechanisms by which these structures form were not revealed. Infrared studies, which will be initiated in several weeks, should help to identify the mechanisms. A tentative mechanism is shown in Figure 9. Carbon monoxide adsorbs as a formate or formate ion by interacting with a surface OH. The formate reacts with a second OH to form the carbonate or reacts with several OH groups to form the methoxide.

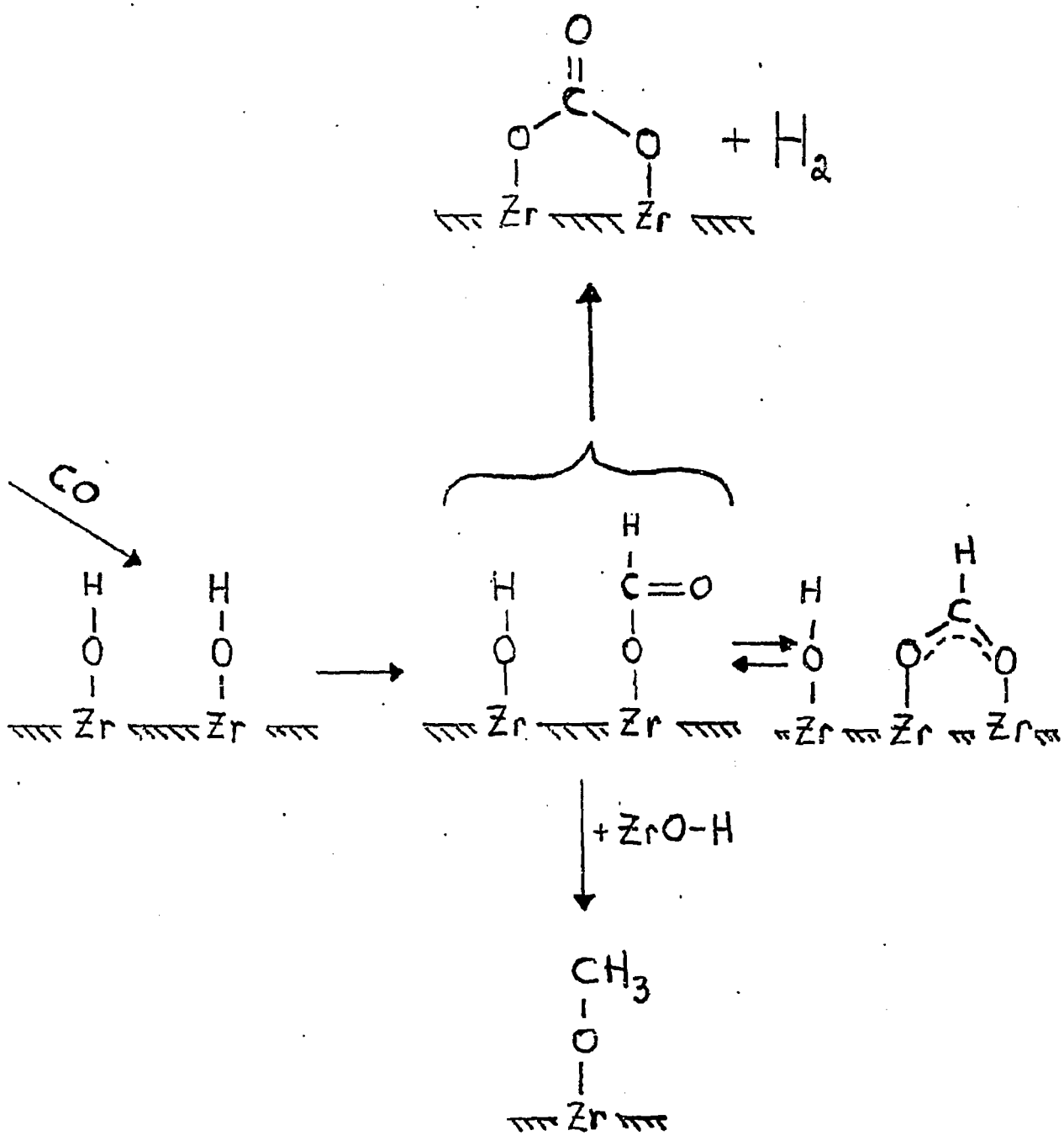

FIGURE 9

Publications resulting from this grant

In print

1. "Study of Fischer-Tropsch Synthesis over Fe/SiO_2: Reactive Scavenging with Pyridine and Cyclohexene" (with C. J. Wang). J. Catal. 80, 172 (1983).

Submitted for publication

1. "The Conversion of Synthesis Gas Over Zirconia" (with M. A. Barker). J. Catal. (submitted).

Manuscripts in preparation

1. "Studies of the Fischer-Tropsch Propagation Reaction over Fe/SiO_2," (with C. J. Wang). intended for submission to J. Catal. by 4/8/83.

2. "Temperature Programmed Studies of Synthesis Gas Adsorption on ZrO_2," (with M.-Y. He). intended for submission to J. Catal. by 4/22/83.

Manuscripts which should be submitted prior to the end of the grant period

1. "Infrared Study of Synthesis Gas Adsorption on ZrO_2," (with M.-Y. He).

2. "Reactive Scavenging of Alkyl Species Over Ruthenium During Fischer-Tropsch Synthesis," (with K. A. Anderson).

REFERENCES

1. Ekerdt, J. G., and Bell, A. T., J. Catal. 62, 19 (1980).
2. Baker, J. A., and Bell, A. T., J. Catal. 78, 165 (1982).
3. Wang, C. J., and Ekerdt, J. G. J. Catal. 80, 172 (1983).
4. Barker, M. A., and Ekerdt, J. G., J. Catal. (submitted for publication).
5. He, M.-Y., and Ekerdt, J. G. (manuscript in preparation).
6. Wang, C. J., and Ekerdt, J. G. (manuscript in preparation).
7. Bell, A. T. (personal communication).
8. Arakawa, H., and Bell, A. T., Ind. Eng. Chem. Process Des. Dev. 22, 97 (1983).
9. Kellner, C. S., and Bell, A. T., J. Catal. 70, 418 (1981).
10. Biloen, P., and Sachtler, W.M.H., Adv. in Catal. 30, 163 (1981).
11. Bell, A. T., Catal. Rev. Sci. and Eng. 23, 203 (1981).
12. Henrici-Olivé, G., and Olivé, S., J. Mol. Catal. 16, 111 (1982).
13. Satterfield, C. N., and Huff, G. A., J. Catal. 73, 187 (1982).
14. Krebs, H. J., Bonzel, H. P., Schwarting, W., and Gafner, G., J. Catal. 72, 199 (1981).
15. Pichler, H., and Ziesecke, K-H., Bureau of Mines Bull. 448 (1950).
16. Cohn, E. M., in "Catalysis" (P. H. Emmett, Ed.) Vol. 4, p. 443, Reinhold, New York, 1956.
17. Storch, H. H., Golumbic, N., and Anderson, R. B., "The Fischer-Tropsch and Related Synthesis," Wiley, New York, 1951.
18. Chang, C. D., Lang, W. H., and Silvestri, A. J., J. Catal. 56, 268 (1979).
19. Chang, C. D., and Silvestri, A. J., J. Catal. 47, 249 (1977).
20. Kaeding, W. W., and Butter, S. A., J. Catal. 61, 155 (1980).
21. Derouane, E. G., Nagy, J. B., Dejaifve, P., van Hooff, J.H.C., Speckman, B. P., Vedrine, J. C., and Naccache, C., J. Catal. 53, 40 (1978).
22. Chang, C. D., and Chu, C.T-W., J. Catal. 74, 203 (1982).
23. Anderson, J. R., Mole, T., and Christov, V., J. Catal. 61, 477 (1980).

24. Dejaifve, P., Vedrine, J. C., Bolis, V., and Derouane, E. G., J. Catal. 63, 331 (1980).

25. Ko, E. I., Benziger, J. B., and Madix, R. J., J. Catal. 62, 264 (1980).

26. Tret'yakov, N. E., Pozdyakov, D. V., Oranskaya, O. M., and Filiminov, V. N., Russ. J. Phys. Chem. 44, 496 (1970).

27. Pichat, P., Veron, J., Claudel, B., and Mathieu, M. V., J. Chim. Phys. 63, 1026 (1966).

28. Courdurier, G., Claudel, B., and Faure, L., J. Catal. 71, 213 (1981).

29. Tanaka, K., and White, J. M., J. Phys. Chem. 86, 3977 (1982).

30. Tanaka, K., and White, J. M., J. Phys. Chem. 86, 4708 (1982).

APPENDIX I

The Conversion of Synthesis Gas Over Zirconia

by

Mitchell A. Barker and John G. Ekerdt

Department of Chemical Engineering
University of Texas at Austin
Austin, Texas 78712

Running Title: Conversion of Syngas Over ZrO_2

Submitted to: Journal of Catalysis

Mail correspondence to: John G. Ekerdt
Department of Chemical Engineering
University of Texas at Austin
Austin, Texas 78712

ABSTRACT

The conversion of synthesis gas was studied over ZrO_2 at 35 atm in a differential reactor in which carbon monoxide conversion never exceeded 2.5%. Isobutene was the major C_4 product. 1-Butene was the major linear C_4 olefin despite its low thermodynamic stability. The constancy of the iso/normal C_4 ratio with residence time and temperature combined with 1-butene isomerization studies suggests that isobutene and 1-butene are primary product and are formed from a common intermediate. A possible reaction mechanism is discussed.

I. INTRODUCTION

The Isosynthesis process refers to the selective conversion of synthesis gas into branched aliphatic hydrocarbons over oxides. The most active oxides are thoria and zirconia (1) which catalyze the formation of hydrocarbons containing four to eight carbon atoms, with isobutane as the major product. The reaction requires high pressure, 30-600 atm (one atm equals 101.3 KPa), and high temperatures, 375 to 475°C.

Little is known about the reaction. The earliest research was conducted in the 1940's (1). The effects of oxide composition and synthesis conditions are reported and mechanisms proposed (1,2,3). The mechanisms involved oxygenated intermediates in which an intermediate ether or alcohol are formed and subsequently dehydrated to an olefin. These proposed mechanisms relied on the acid/base nature of the catalytically active oxides. The details of the mechanisms were not given, merely the stoichiometry of the reactions. The majority of the early work concentrated on thoria because it was the most active catalyst. Recently, Chang et al. (4) reported isosynthesis results over ZrO_2. This study was not specifically directed toward the isosynthesis reaction; therefore, the reaction mechanism was not discussed.

Zirconia has weak basic sites (5-9), Lewis acid sites (6,10-12) and possibly some Brønsted sites (11). Zeolites, notably ZSM-5, have acid sites which catalyze the conversion of methanol into branched hydrocarbons (13). Dimethyl ether (DME) is an intermediate product for the methanol conversion reaction. Dimethyl ether is also generated during isosynthesis over ThO_2 (1) and ZrO_2 (1,4), and has been proposed as an intermediate product because it reacts over ZrO_2 and ThO_2 in the presence of H_2 to give isobutane (1). Mechanisms for the acid catalyzed conversion of

methanol/DME over ZSM-5 zeolites have been proposed (13-18) some of which consider ether and alcohol intermediates. The presence of acid sites and a common intermediate product suggest that isosynthesis and methanol conversion may have some reactions which are identical.

This study investigated the isosynthesis reaction over ZrO_2. Zirconia is the second most active isosynthesis catalyst (1), yet little is known about CO/H_2 products or reactions over it. The formation of C_4 products was studied at low conversion to gain insight into the primary reaction mechanisms.

II. METHODS

The isosynthesis reaction was studied in a high pressure microreactor built from 6.35 mm OD 304 stainless steel tubing. The catalyst bed of 1-3μ ZrO_2 spheres, which was approximately 100 mm deep, was supported by a region of quartz fiber and a 200 mesh stainless steel screen. A 1.59 mm OD stainless steel sheathed thermocouple was inserted axially into the reactor; the tip was located in the lower third of the catalyst bed. The reactor was wrapped with heating tape. The heating zone extended 20 mm on either end of the catalyst bed. Reactants were preheated in the section of tubing above the catalyst bed.

The 1-butene isomerization reaction was studied in a 12.70 mm OD quartz tube fitted with a quartz frit which served as the catalyst support. Cajon Ultra-Torr fittings provided the transition between the quartz and stainless steel tubing.

A schematic of the experimental apparatus is presented in Figure 1. The entire system was built with stainless steel. The gas flowrates and reactor pressure were controlled with metering valves. Reactor effluent was

reduced in pressure to one atmosphere and vented through a gas chromatograph sample valve.

The reactor effluent was analyzed by a gas chromatograph fitted with a flame ionization detector. A 3.18 mm OD x 6.1 m stainless steel OV-101 column was used to separate CH_4, C_2H_4, C_2H_6, the C_3's, i-C_4H_{10}, i-C_4H_8 and 1-C_4H_8, cis-2-C_4H_8, and trans-2-C_4H_8. Propane and propene eluted at the same time as did iso- and 1-butene. Iso-butene and 1-butene were separated using a 3.18 mm OD x 1.83 m nickel column packed with Carbowax W containing 0.19 percent picric acid. The OV-101 column is referred to as GC method 1 and the Carbowax W column as GC method 2.

All the isosynthesis experiments were performed at 35 atm. Prior to an experiment the reactor was purged with hydrogen and the temperature and gas flows were adjusted. The reactants were directed through the reactor and a the effluent concentration was determined after a minimum of 20 reactor residence times (reactor volume/volumetric feed rate evaluated at the inlet conditions) had passed. This was done to ensure steady state activity had been reached. Occasionally a second analysis was performed 30 minutes later; in each case the second analysis indicated that steady state had been reached at the first sampling time. Following each experiment the reactor was flushed with hydrogen and stored under hydrogen at 35 atm.

The zirconia (Alfa-Ventron) was 98.9 percent pure. It was supplied as a 1-3 μ powder and was used without further treatment. The powder had a BET area of 5.81 m^2/gm.

The hydrogen had a minimum purity of 99.98 mole percent and was used without further purification. Carbon monoxide (Matheson) had a minimum purity of 99.8 mole percent and was passed through a 75 cm^3 bed of 4A molecular sieves maintained at 130°C to decompose any metal carbonyls.

1-Butene was supplied as a mixture with helium. Gas chromatograph analysis indicated it contained 230 ppm 1-butene, 2 ppm cis-2-butene, 4 ppm trans-2-butene, 3 ppm isobutane and the balance helium.

III. RESULTS

Products from Synthesis Gas

The product distributions reflect kinetic as well as mass transfer effects. Intraparticle transport is not an issue because the 1-3 μ ZrO_2 particles were nonporous. Mass transfer limitations between the bulk gas phase and the catalyst surface is strongly suggested by the Arrhenius plot shown in Figure 2. The ordinate is based on the moles of CO reacted to C_1 to C_4 hydrocarbons and the assumption that the concentration of CO and H_2 is constant. (Carbon monoxide conversion never exceeded 2.5 percent.) The slope of the upper curve, ZrO_2, declines rapidly above 440°C, the slope corresponding to 9.7 Kcal/mole. This implies that above 440°C bulk phase diffusion, which generally has an activation energy less than 5 Kcal/mole, is strongly influencing the rate. The altered slope reflects the transition from surface reaction to bulk diffusion control. This limitation is not unreasonable because the particle Reynold's number was approximately 5×10^{-3} over the range of flowrates and temperatures employed. Alternately, the mechanism or surface rate controlling step may be different above 440°C. It was not possible to determine the cause for the altered activation energy with the reactor used for these studies.

Temperature gradients between the bulk gas phase and catalyst surface could not be determined from the data. They were probably nonexistent because the conversion was maintained below 2.5 percent, thereby limiting the generation of thermal energy by chemical reaction. Temperature

gradients along the length of the catalyst bed were not observed. However, a temperature gradient probably existed between the center of the catalyst bed and the tube wall because the heat was supplied through the tube wall and because the gas flow was laminar. The extent to which any difference between the average temperature and centerline temperature affected the rate and reported activation energies could not be determined. This introduces uncertainty and the absolute value of the activation energies reported herein may not be correct; however, the magnitudes and trends are representative of isosynthesis over ZrO_2.

Under certain reaction conditions, blank activity became significant. The blank activity was caused by the catalytic activity of the stainless steel reactor walls. The surface area of the reactor walls represented about 0.2 percent of the surface area of the zirconia. The blank effect was accentuated by the low activity of the zirconia. Figure 2 also contains an Arrhenius plot of the blank activity. At 300°C there was a ten-fold difference in activity, while at 450°C activity represented about 5 percent of the total amount of CO reacted. To compensate, each run was done with and without catalyst at a common residence time and the blank activity was subtracted out on an individual hydrocarbon basis. Table 1 presents a product comparison of the blank and zirconia plus blank activity. Note that most of the blank activity involves methane through propane. This is in accordance with the large amount of methane formed during CO reduction over iron at high temperature and pressure (2). The quantity of C_4 products from the blank activity was minimal and thus adds to the reliability of the analysis of the C_4 products over zirconia.

The product distribution as a function of temperature is represented in Figure 3. These data were taken at a feed rate of 75 scc/min, hence the

residence time will vary with temperature. Figure 4 is a plot of the effect of feed rate on the products formed. The effect is a weak one, therefore the changes in product distributions seen in Figure 3 can be attributed to the changes in temperature. Although experiments were conducted as low as 250°C and up to 550°C, only the data from 325 to 450°C are shown. Below 325°C it was felt that the background activity was too large, and above 450°C diffusional effects dominated. This is an interesting temperature range though since it begins close to the temperature at which the first hydrocarbons were detected, 275°C. In addition to the products shown in Figure 10, dimethyl ether (DME) was also formed. Its presence was noted but not quantified.

As the temperature increased the percent methane increased and the percent C_4's decreased, indicating the rate of methane formation increased faster than the rate of propagation. Another possibility is that the C_1 species used for building hydrocarbons is formed by a different reaction than is methane. The percentage of C_2's and C_3's in the product remained fairly constant.

The amounts of each product remained relatively constant with feed rate (residence time). There was a slight increase in methane and decrease in C_4's at the lowest feed rate. It is doubtful that this behavior was due to a changing mass transfer coefficient because of the low particle Reynold's numbers (19). Causes for the changes were not revealed in the present study.

Apparent activation energies for the saturated and unsaturated compounds were determined from individual Arrhenius plots. The results are listed in Table 2. Methane, ethane and the butanes have nearly equal activation energies. The unsaturated compounds have lower values. The

similarity of activation energies may imply that product forming reactions for the saturated compounds are similar, as are the product forming reactions for the unsaturated compounds.

One of the most important features of the isosynthesis is the predominant production of branched hydrocarbon products. Figure 5 shows the distribution of C_4 isomers versus temperature. For clarity the curves for the cis and trans isomers, and for the n-butane are shown separately. For the purposes of this figure the percentages of cis- and trans-2-butene can be considered equal; therefore they are represented by one curve. Unfortunately, the GC method, method 1, used for the majority of points in this plot, did not separate 1-butene from iso-butene. The second GC method did resolve these two compounds, but the reactor effluent was analyzed at only three reaction temperatures. These points have been included in Figure 5. The second method demonstrated that the iso-butene/1-butene curve is mainly iso-butene. The 1-butene remained between 10 and 15 percent of the total C_4's formed. The limited points determined by the second GC method limits quantitative comparisons between the two GC methods.

It is clear that at all temperatures the predominant product was branched, either iso-butane or iso-butene. As the temperature increased, the hydrogenation rate increased and more iso-butene was converted to iso-butane. Similarly, the percentage of n-butane increased with increasing temperature, with a consequent decrease in the percent of 1- and 2-butenes in the product. Table 3 details the data taken by the second GC method. The ratio of unsaturated to saturated C_4's declined with increasing temperature, consistent with the increase in hydrogenation rate mentioned above. The iso to normal ratio was constant over the temperature range shown. The preponderance of branched products at all temperatures might

lead one to believe that it is a primary product as opposed to being the result of an isomerization reaction. To study this, the space velocity was varied while monitoring the distribution of the C_4 isomers. The results are shown in Figure 6 and Table 4. Once again, the upper curve represents both iso-butene and 1-butene.

The plot shows that at high residence times the amount of iso-butane increased while the percent 1-butene and/or iso-butene decreased. Based on the data in Table 4 and Figure 5 it is safe to assume that the longer residence times led to increased hydrogenation of iso-butene, creating more iso-butane. The slight increase in n-butane at long residence times was the result of hydrogenation of the linear butenes. The above discussion assumes that the 1-butene was not undergoing skeletal isomerization; this will be discussed in a later section. The constancy of the iso to normal ratio at varying space velocities and temperatures suggests that the mechanism for branched and linear products is the same; the branched products being preferred due to steric or kinetic effects.

The concentrations of the linear olefins formed during isosynthesis have been normalized and are shown in Tables 3 and 4. The mole fraction of each linear olefin, when in equilibrium with each other is shown for comparison. Equilibrium values were calculated from free energy of formation data (20). In all cases the linear olefins formed show a significant deviation from the equilibrium values. The deviation decreased at higher temperatures and longer residence times. There was always more 1-butene and less 2-butene than there would be at equilibrium. Apparently, the 1-butene is the initial linear olefin formed and the cis- and trans-2-butenes are formed by double bond isomerization of the 1-butene. The cis and trans isomers are close to being in equilibrium with each other

as would be expected at the temperatures used. The reactions of the linear olefins will be discussed further in the following section.

Reactions of 1-Butene

1-Butene was fed as a mixture with helium the concentration, 115 to 150 ppm, was chosen to approximate the concentration of C_4's found during isosynthesis. Isomerization and hydrogenation activity was studied at 35 atm in the stainless steel reactor and at 1 atm in the quartz reactor. The stainless steel tube wall catalyzed double bond migration and hydrogenation; the quartz surface was inert.

The results at 35 atm are presented in Table 5. Isobutene is thermodynamically favored, however skeletal isomerization of 1-butene to iso-butene was not observed. The linear olefins were completely equilibrated in the presence of H_2. Double bond migration was inhibited in the presence of CO. The blank activity was not subtracted from the 1-butene results presented in Table 5; therefore, these results can only be used to make qualitative comments. Comparing the isomerization results with the isosynthesis results suggests that iso-butene is not formed from 1-butene and that CO or its adsorbed forms(s) inhibits equilibration of linear olefins during isosynthesis.

At 1 atm zirconia did not catalyze olefin hydrogenation. Double bond migration was observed when 1-butene and hydrogen contacted the catalyst. The linear olefins did not equilibrate at this pressure; isomerization activity increased with temperature. These results suggest that high hydrogen pressure is required to affect hydrogenation.

IV. DISCUSSION

The distribution of branched/normal C_4's remained constant with residence time and temperature. Increasing the residence time or temperature increased the alkane/olefin distribution and the degree of isomerization of 1-butene into the internal olefins. In addition, isobutene was the major C_4 olefin. These results strongly suggest that iso-butene and 1-butene are the primary C_4 products and that they are formed from a common surface intermediate.

More experiments are required before the mechanism by which C_4's are formed can be proposed and defended. A realization that the surface is acidic and that dimethyl ether was observed can be used to suggest a possible mechanism. This mechanism involves stepwise addition of a C_1 species to a C_3 species. The C_3 species is most likely a carbenium ion because the predominant product is branched and the most stable C_3 favoring this would be a secondary carbenium ion.

Dimethyl ether, noted but not quantified in this study, has been seen elsewhere along with methanol (1,4). Their appearance at only low conversion and moderate temperatures has suggested that they are intermediate products. The retention of the carbon-oxygen bond in these intermediate species suggests that CO does not dissociate upon adsorption. Carbon monoxide and carbon dioxide form carbonates and formates over thoria (21) while CO_2 has been found to form carbonates over zirconia (10). Adsorption/desorption and temperature programmed reaction studies of CO and H_2 suggest that CO adsorbs as a formate and is subsequently reduced to a methoxy on ZrO_2 at 1 atm (22). Only methane was detected at 1 atm (22), the means by which the formate or methoxy form a stable C_1 or C_2 oxygenated product at elevated pressures was not revealed.

Passage of DME over thoria at 30 atm or zirconia (no pressure was given) produced iso-C_4 hydrocarbons. Diethyl ether did not produce iso-C_4 hydrocarbons over thoria (1). Zeolites, notably ZSM-5, catalyze the conversion of methanol into DME and iso-C_4 hydrocarbons (13). Mechanisms leading to an iso-C_4 which involve an oxygenated and a nonoxygenated intermediate have been proposed over the zeolite. Either the protonated form of methanol or DME add a methyl group to propylene (14,17) or the C_3 carbenium ion is methylated by methanol or DME through the initial formation of a higher ether (15,18). These same mechanisms could be present during isosynthesis over the acid sites of ZrO_2 with DME serving as the source of C_1 species. Alternately, a C_1 intermediate formed directly from CO may be the C_1 source rather than a gas phase product such as DME.

The means by which C_2 and C_3 hydrocarbons and surface species are formed, stepwise surface formation versus secondary reaction between an intermediate product and a surface species, are not revealed by the present study. A common precursor to butenes and ethylene is suggested by their similar activation energy. The isosynthesis mechanisms are currently under investigation.

ACKNOWLEDGEMENT

This work was supported by the Division of Chemical Sciences, Office of Basic Energy Sciences, U.S. Department of Energy under Contract DE-AS05-80ER1072. The University of Texas Center for Energy Studies provided support for the gas chromatograph.

REFERENCES

1. Pichler, H., and Ziesecke, K-H., Bureau of Mines Bull. 448 (1950).

2. Storch, H. H., Golumbic, N., and Anderson, R. B., "The Fischer-Tropsch and Related Synthesis," Wiley, New York, 1951.

3. Cohn, E. M., in "Catalysis" (P. H. Emmett, Ed.), Vol. 4, p. 443, Reinhold, New York, 1956.

4. Chang, C. D., Lang, W. H., and Silvestri, A. J., J. Catal. 56, 268 (1979).

5. Yamaguchi, T., Nakano, Y., Iizuka, T., and Tanabe, K., Chem. Lett. 667 (1976).

6. Yamaguchi, T., Nakano, Y., and Tanabe, K., Bull. Chem. Soc. Japan 51, 2482 (1978).

7. Canesson, P., and Blanchard, M., J. Catal. 42, 205 (1976).

8. Yamaguchi, T., Sasaki, H., and Tanabe, K., Chem. Lett. 1017 (1973).

9. Siegel, V. H., Schollner, R., Dombrowski, D., and Wendt, G., Z. Anorg. Allg. Chem. 441, 252 (1978).

10. Tret'yakov, N. E., Pozdyakov, D. V., Oranskaya, O. M., and Filiminov, V. N., Russ. J. Phys. Chem. 44, 596 (1970).

11. Nakano, Y., Iizuka, T., Hattori, H., and Tanabe, K., J. Catal. 57, 1 (1979).

12. Lunina, E. V., Selivanooskii, A. K., Golubev, V. B., Samgina, T. Y., and Markaryan, G. I., Russ. J. Phys. Chem. 56, 247 (1982).

13. Chang, C. D., and Silvestri, A. J., J. Catal. 47, 249 (1977).

14. Kaeding, W. W., and Butter, S. A., J. Catal. 61, 155 (1980).

15. Derouane, E. G., Nagy, J. B., Dejaifve, P., van Hooff, J.H.C., Speckman, B. P., Vedrine, J. C., and Naccache, C., J. Catal. 53, 40 (1978).

16. Chang, C. D., and Chu, C.T-W., J. Catal. 74, 203 (1982).

17. Anderson, J. R., Mole, T., and Christov, V., J. Catal. 61, 477 (1980).

18. Dejaifve, P., Vedrine, J. C., Bolis, V., and Derouane, E. G., J. Catal. 63, 331 (1980).

19. Chambers, R. P., and Boudart, M., J. Catal. 6, 141 (1966).

20. Stull, D. R., Westrum, E. F., and Sinke, G. C., "The Chemical Thermodynamics of Organic Compounds," Wiley, New York, 1969.

21. Coudurier, G., Claudel, B., and Faure, L., J. Catal. 71, 213 (1981).

22. He, M.-Y., and Ekerdt, J. G., unpublished results.

List of Tables

Table 1 Comparison of Blank and Blank plus Zirconia Activity

	Blank 360°C 100 scc/min 35 atm (ppm)	Blank plus Zirconia 360°C 75 scc/min 35 atm (ppm)
Methane	170	1100
Ethylene	36	90
Ethane	7	34
Propane/Propene[(a)]	12	50
iso-Butane	0	10
iso/1-Butene[(a)]	5	135
n-Butene	0	2
trans-2-Butene	0	11
cis-2-Butene	0	11

(a) The GC method used for the data in this table did not separate these compounds

Table 2 Apparent Activation Energies for Individual Compounds

	Activation Energy (Kcal/mole)
Methane	27.7
Ethylene	17.8
Ethane	28.4
Butenes	12.1
Butanes	28.3

Table 3 Detailed Analysis of Butanes and Butenes as a Function of Temperature

$CO/H_2 = 1$
Pressure 35 atm
Feed Rate 100 scc/min
3.6 gm Zirconia

	330 C	360 C	405 C
iso-Butane	0.034	0.061	0.180
iso-Butene	0.687	0.639	0.593
1-Butene	0.113	0.127	0.105
n-Butane	0.026	0.024	0.033
trans-2-Butene	0.085	0.085	0.080
cis-2-Butene	0.055	0.063	0.060
iso/normal	2.58	2.34	2.57
Butenes/Butanes	15.7	10.7	3.68
Normalized Linear Olefin Distribution			
1-Butene	0.447	0.462	0.429
trans-2-Butene	0.336	0.309	0.327
cis-2-Butene	0.217	0.229	0.245
Predicted Linear Olefin Distribution at Equilibrium			
1-Butene	0.168	0.180	0.204
trans-2-butene	0.515	0.504	0.484
cis-2-butene	0.317	0.315	0.313

Table 4 Detailed Analysis of Butanes and Butenes as a Function of Feed Rate

CO/H_2 = 1
Pressure 35 atm
Temperature 365 C
3.6 gm Zirconia

	33 scc/min	60 scc/min	100 scc/min
iso-Butane	0.244	0.175	0.061
iso-Butene	0.462	0.531	0.639
1-Butene	0.086	0.108	0.127
n-Butane	0.046	0.037	0.024
trans-2-Butene	0.093	0.083	0.085
cis-2-Butene	0.069	0.066	0.063
iso/normal	2.40	2.40	2.34
Butenes/Butanes	2.45	3.72	10.7
Normalized Linear Olefins			Equil. at 365 C
1-Butene	0.347	0.420	0.462	0.180
trans-2-Butene	0.375	0.323	0.309	0.504
cis-2-Butene	0.278	0.257	0.229	0.315

Table 5 Effect of Feed Composition on 1-Butene Isomerization

Pressure 35 atm
Temperature 365 C
Feed Rate 100 scc/min
3.6 gm Zirconia

	CO/H_2 [a]		CO/1-Butene [b]		H_2/1-Butene [c]	
	ppm	mol frac	ppm	mol frac	ppm	mol frac
iso-Butane	55	0.061	5	0.035	3	0.019
iso-Butene	578	0.639	5	0.035	2	0.010
1-Butene	115	0.127	44	0.354	23	0.144
n-Butane	22	0.024	2	0.012	27	0.173
trans-2-Butene	57	0.085	40	0.319	61	0.394
cis-2-Butene	77	0.063	31	0.245	40	0.259
Normalized Linear Olefins						
1-Butene		0.462		0.386		0.181
trans-2-Butene		0.309		0.347		0.494
cis-2-Butene		0.229		0.267		0.325

(a) 1:1 $CO:H_2$ in the feed

(b) 50%:115 ppm CO:1-butene in the feed

(c) 50%:150 ppm H_2:1-butene in the feed

List of Figures

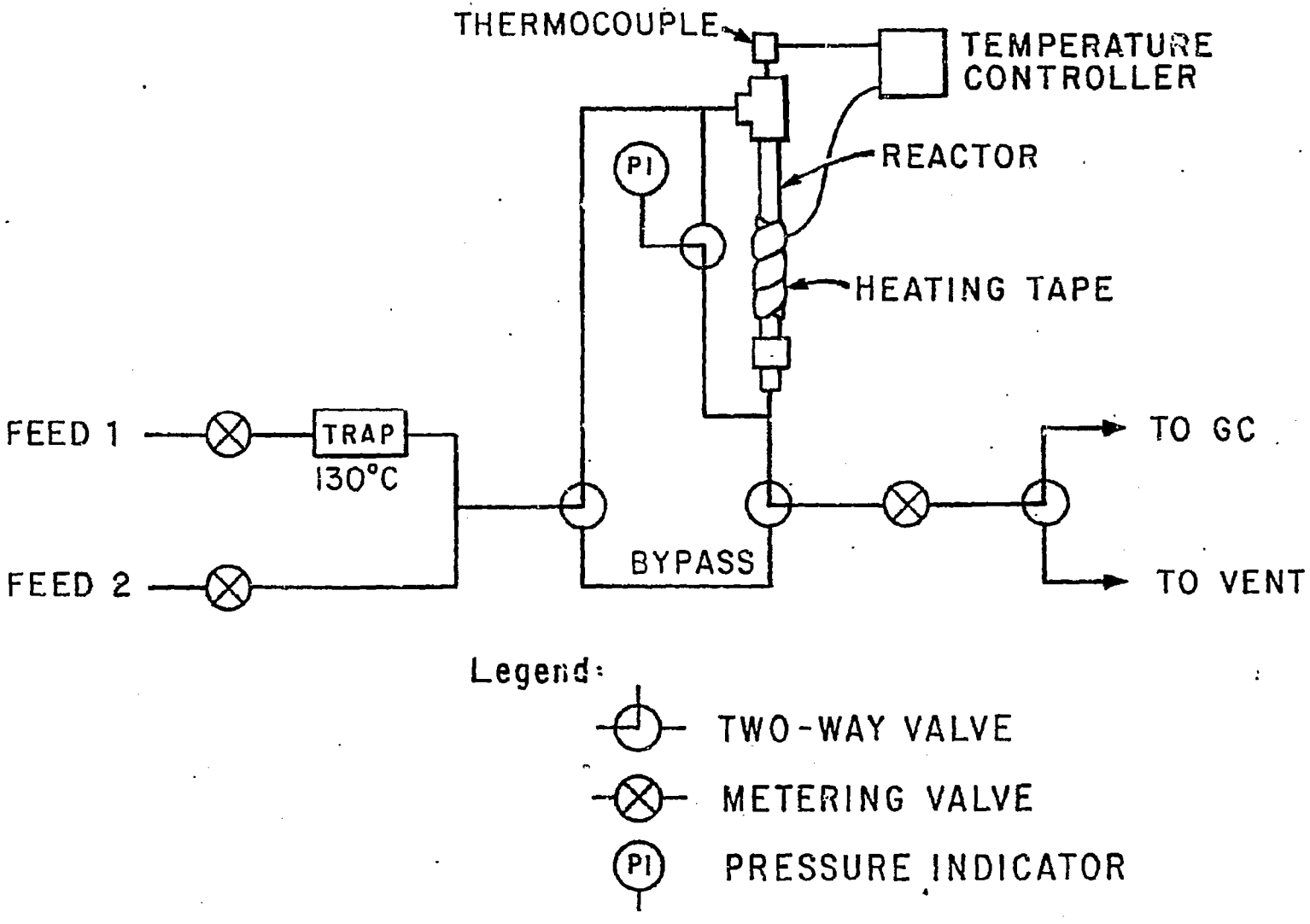
THERMOCOUPLE
TEMPERATURE CONTROLLER
REACTOR
PI
HEATING TAPE
FEED 1
TRAP
130°C
FEED 2
BYPASS
TO GC
TO VENT
Legend:
TWO-WAY VALVE
METERING VALVE
PI
PRESSURE INDICATOR

Figure 1

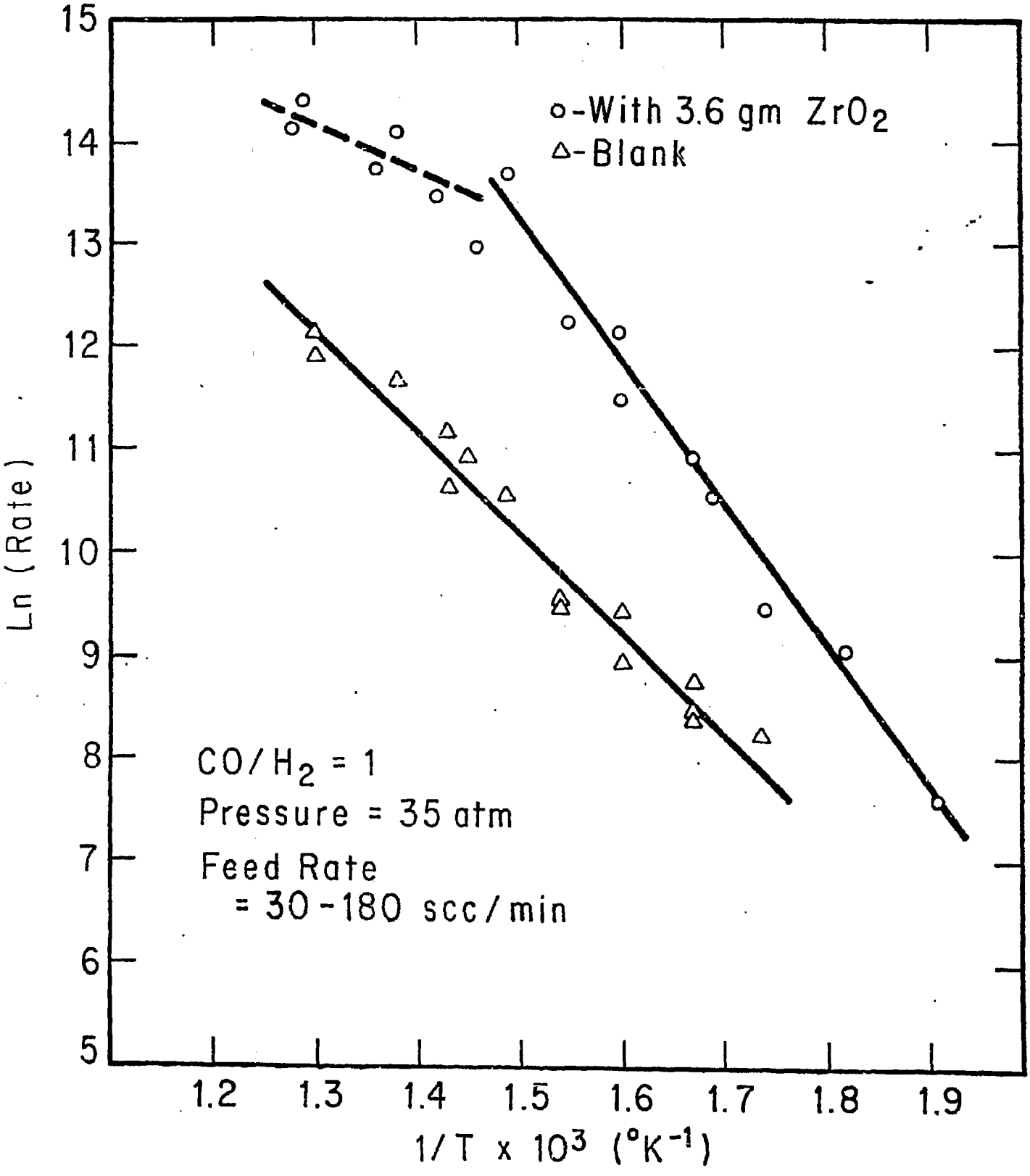
15
14
13
12
11
10
9
8
7
6
5
Ln (Rate)
o-With 3.6 gm ZrO_2
Δ-Blank
$CO/H_2 = 1$
Pressure = 35 atm
Feed Rate
= 30-180 scc/min
1.2
1.3
1.4
1.5
1.6
1.7
1.8
1.9
1/T x 10^3 ($°K^{-1}$)

Figure 2

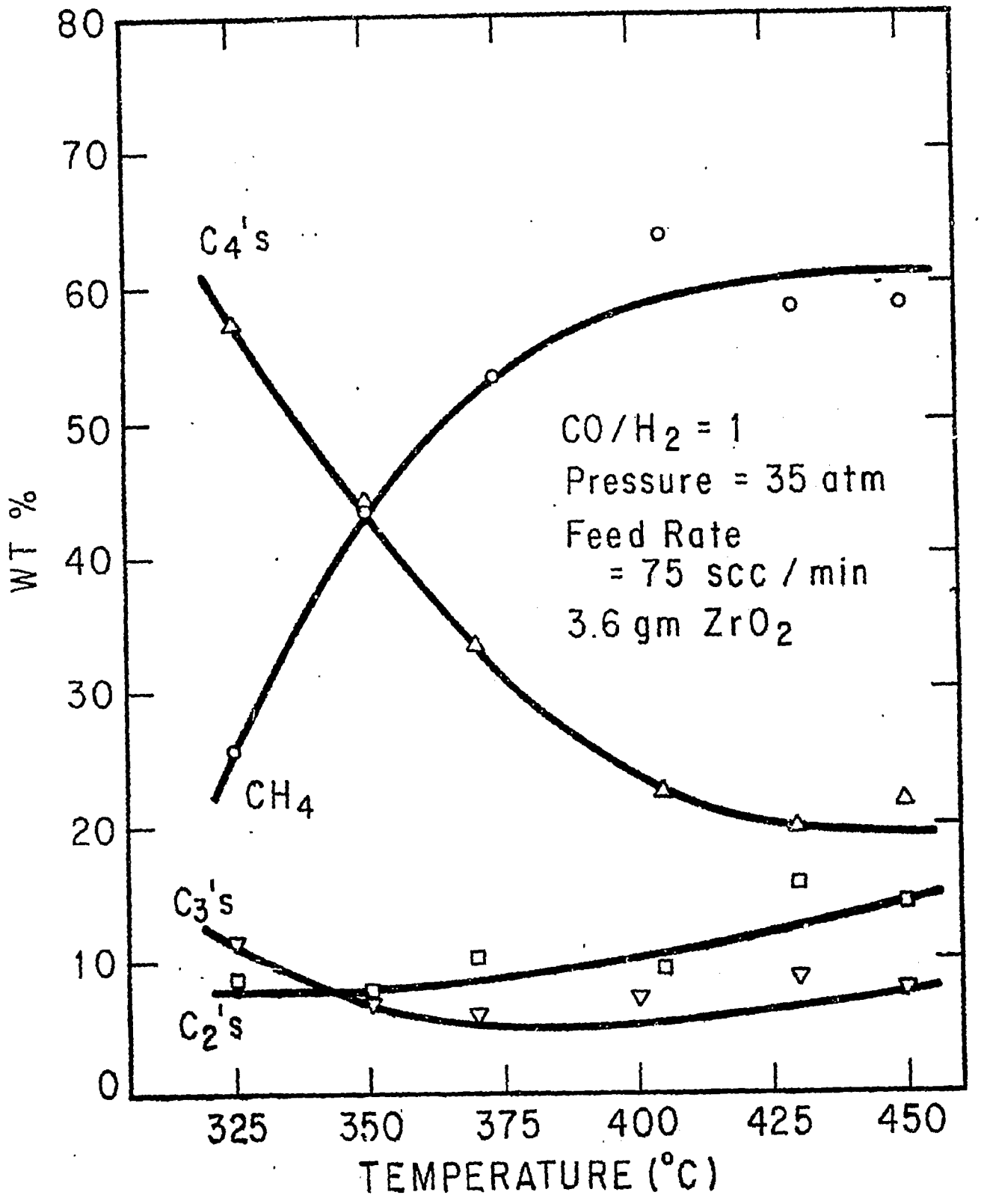
80
70
60
50
40
30
20
10
0
WT %
C4's
CH4
C3's
C2's
CO/H2 = 1
Pressure = 35 atm
Feed Rate
= 75 scc / min
3.6 gm ZrO2
325
350
375
400
425
450
TEMPERATURE (°C)

Figure 3

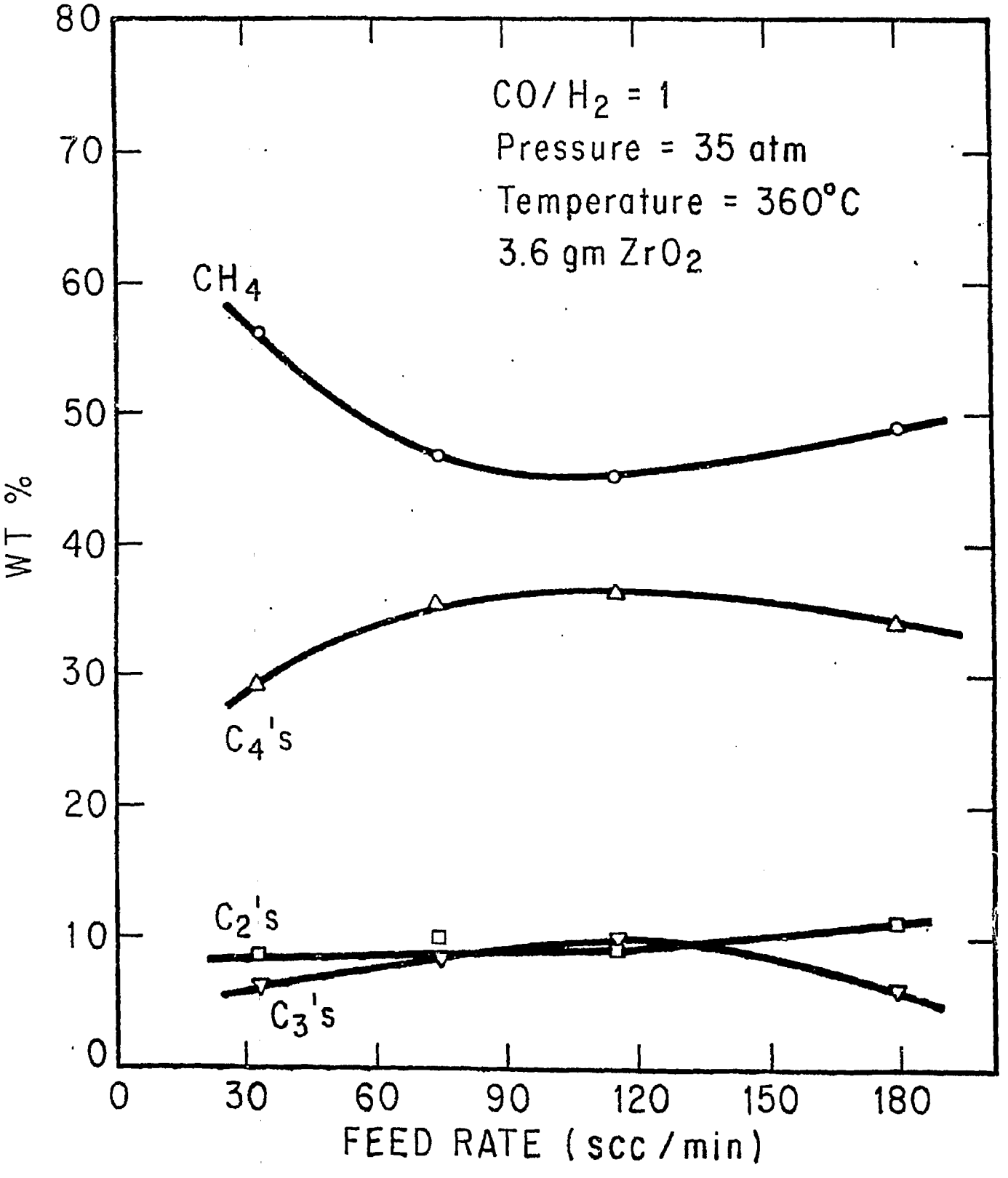
80
70
60
50
40
30
20
10
0
WT %
CO/H2 = 1
Pressure = 35 atm
Temperature = 360°C
3.6 gm ZrO2
CH4
C4's
C2's
C3's
0
30
60
90
120
150
180
FEED RATE (scc/min)

Figure 4

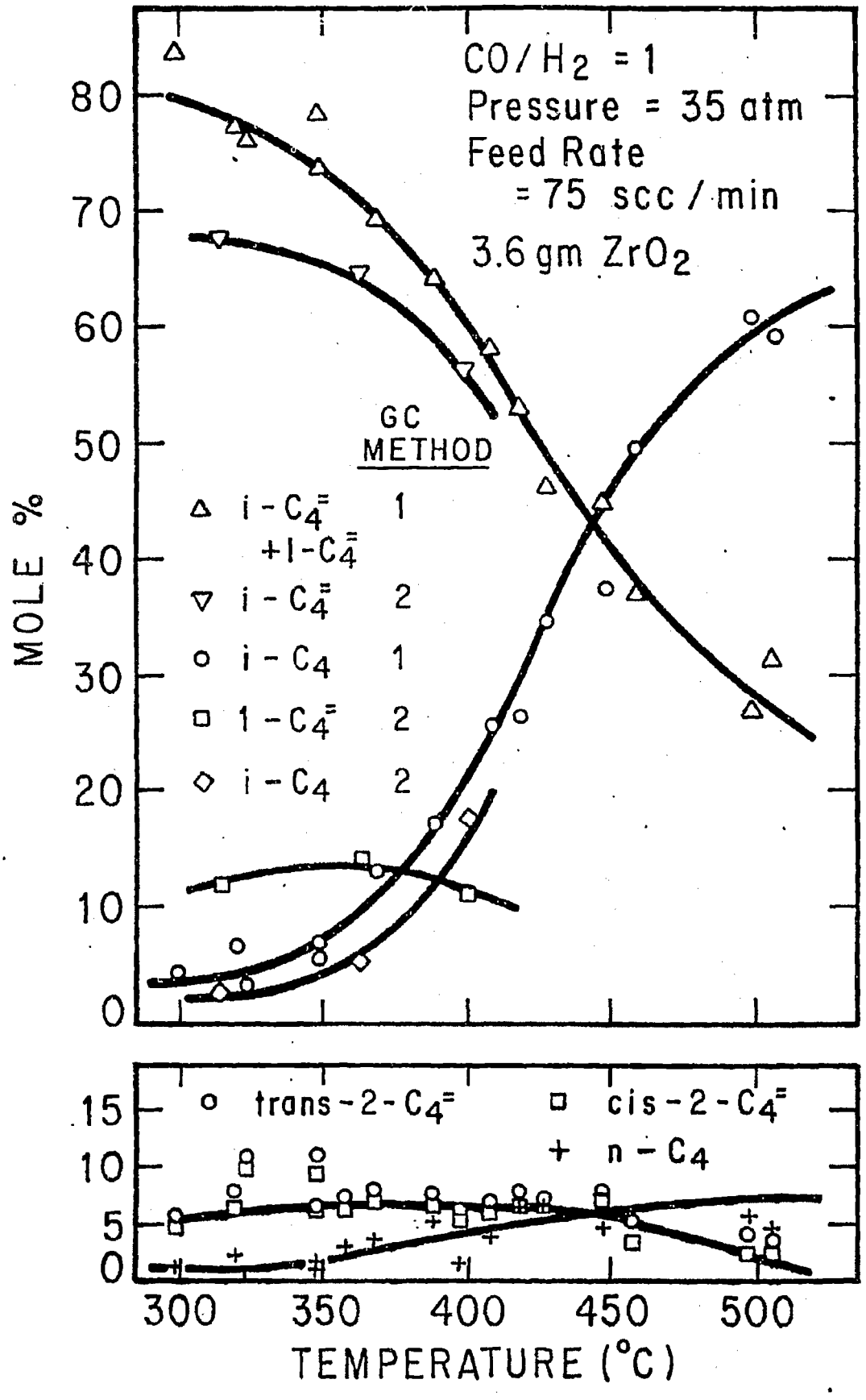
CO/H2 = 1
Pressure = 35 atm
Feed Rate
= 75 scc/min
3.6 gm ZrO2
GC METHOD
Δ i-C4= + 1-C4= 1
▽ i-C4= 2
○ i-C4 1
□ 1-C4= 2
◇ i-C4 2
MOLE %
80
70
60
50
40
30
20
10
0
○ trans-2-C4=
□ cis-2-C4=
+ n-C4
15
10
5
0
300
350
400
450
500
TEMPERATURE (°C)

Figure 5

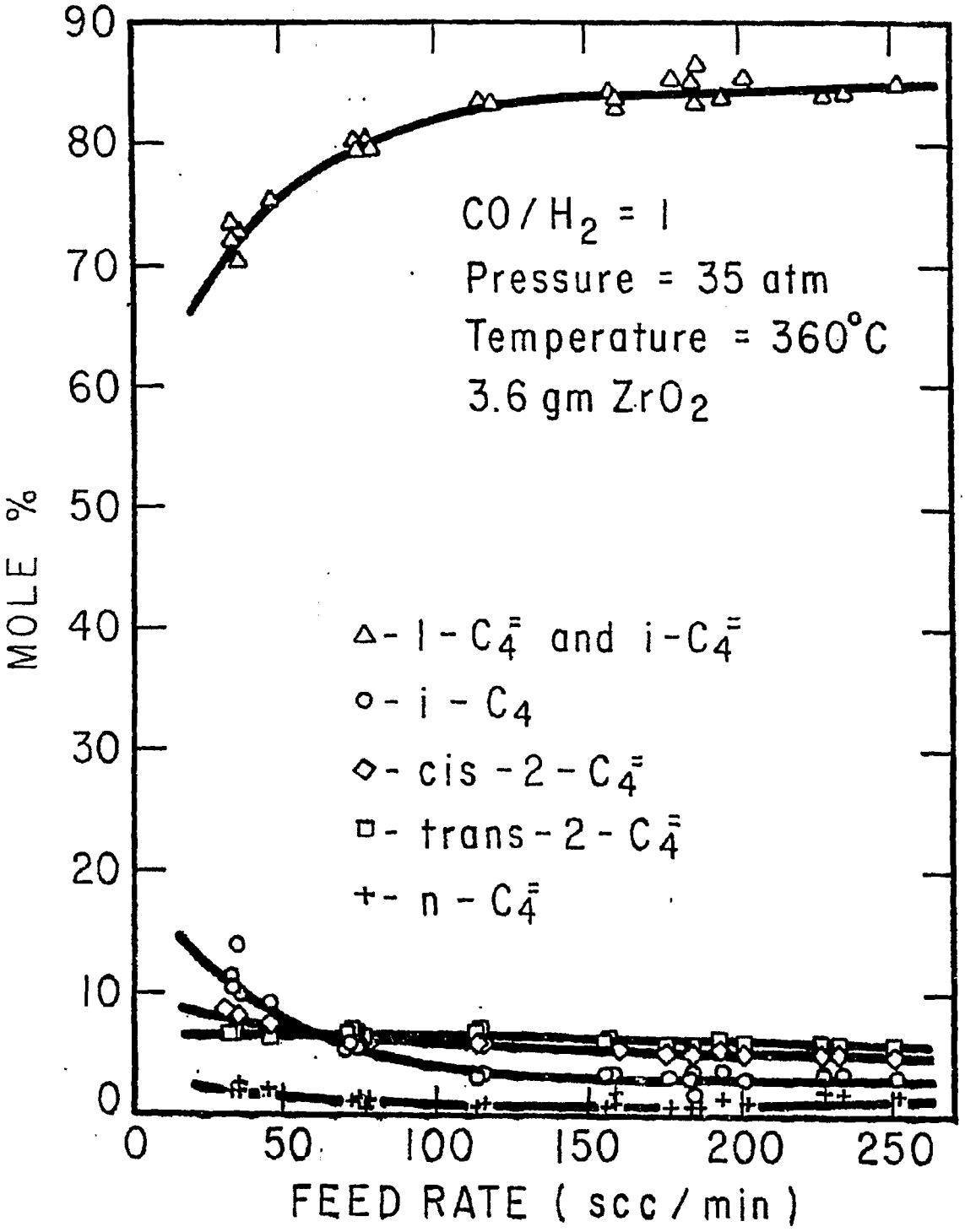
90
80
70
60
50
40
30
20
10
0
MOLE %
0
50
100
150
200
250
FEED RATE (scc / min)
CO / H2 = 1
Pressure = 35 atm
Temperature = 360°C
3.6 gm ZrO2
△- 1 - C4= and i - C4=
○- i - C4
◇- cis - 2 - C4=
□- trans - 2 - C4=
+- n - C4=

Figure 6